Inorganic Chemistry

Article

pubs.acs.org/IC

Bulky N-Phosphino-Functionalized N-Heterocyclic Carbene Ligands: Synthesis, Ruthenium Coordination Chemistry, and Ruthenium Alkylidene Complexes for Olefin Metathesis[⊥]

Christopher C. Brown,*[,†] Frank Rominger,[‡] Michael Limbach,[†] and Peter Hofmann[†,‡]

[†]Catalysis Research Laboratory (CaRLa) and [‡]Organisch-Chemisches Institut, University of Heidelberg, Im Neuenheimer Feld 584, D-69120 Heidelberg, Germany

Supporting Information

ABSTRACT: Ruthenium chemistry and applications in catalytic olefin metathesis based on N-phosphino-functionalized N-heterocyclic carbene ligands (NHCPs) are presented. Alkyl NHCP Ru coordination chemistry is described, and access to several potential synthetic precursors for ruthenium alkylidene complexes is outlined, incorporating both trimethylsilyl and phenyl alkylidenes. The Ru alkylidene complexes are evaluated as potential olefin metathesis catalysts and were shown to behave in a latent fashion. They displayed catalytic activity at elevated temperatures for both ring closing metathesis and ring opening metathesis polymerization.

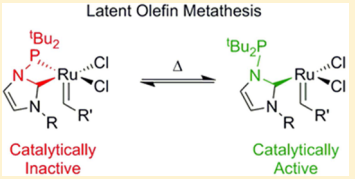

INTRODUCTION

The introduction of the first generation of Grubbs catalysts such as **A**,[1] beginning in the 1990s, proved to be a significant discovery which allowed for the simplification of multistep organic synthesis, for improved selectivities in organic transformations, and the homogeneously catalyzed polymerization of a wide variety of functionalized cyclic olefinic substrates. A large manifold of ruthenium alkylidene complexes for olefin metathesis have been prepared by replacing, for example, one or both of the phosphines with N-heterocyclic carbene ligands (NHCs) (**B**)[2] and pyridines,[3] of the chlorides with bromides, iodides, or pseudohalides such as alkoxides (**C**)[4] or by varying the alkylidene moiety (**D**).[5] The investigation of NHC chelating ligand systems has, however, received significantly less attention. Notable examples include the employment of axially chiral 1,1′-binaphthyl- or 1,1′-biaryl-substituted NHC-ruthenium catalysts for asymmetric olefin metathesis,[6] and the catalysts introduced for Z-selective olefin metathesis by Grubbs et al. featuring NHC ligands with C−H-activated N-adamantyl groups, leading to crowded five-membered chelate complexes (**D**).

Although numerous phosphine functionalized NHC ligands (NHCPs) have been published since the synthesis of the first representative example by Herrmann et al. in 1996,[7] few systems possess electron-rich, bulky dialkyl-substituted phosphino groups.[8] By far, most research related to the use of NHCPs as spectator ligands in transition metal catalysis has focused on cross-coupling reactions. A small number of papers on the ruthenium coordination chemistry of NHCP ligands have been published.[8a,9] Closely related to the present work is, however, a report recently published by our group concerning bulky N-phosphino-methyl functionalized N-heterocyclic carbene chelate ligands.[10] Our report is the only example, to the best of our knowledge, of a study into the catalytic olefin metathesis viability of a ruthenium NHCP system.

Specifically, we have an interest in developing *cis*-chelating analogues of the Grubbs second-generation catalyst system. Our efforts are centered on the use of bidentate bulky ligands to enforce the *cis* binding mode of the donor atoms. We have previously reported on the synthesis, characterization, and catalytic activity of two classes of systems. Our original report centered around dicationic, dinuclear bis(di-*tert*-butylphosphino)methane (dtbpm) ruthenium olefin metathesis catalysts (**F1**). These systems, containing a four-membered bisphosphine chelate structure, showed remarkably high activity in ring opening metathesis polymerization (ROMP), leading to at least an order of magnitude of improvement for ROMP of substrates such as *cis*-cyclooctene and cyclopentene. The mechanistic details of these efficient ROMP-catalysts were investigated and deciphered both in the solution and in the gas phase.[11] In the course of our bisphosphine studies, the five-membered bidentate bisphosphine bis(di-*tert*-butylphosphino)-ethane (dtbpe) system was also employed, leading to (**F2**), which showed a decrease in activity when compared to the related dtbpm system **F1**.[10] Such bisphosphines may be considered the *cis*-phosphine coordination analogues of first generation Grubbs catalysts (**A**).

We also investigated a new series of structurally related potential olefin metathesis catalyst precursors with mixed bidentate N-heterocyclic carbene−phosphine ligand systems (**E**).[10] The NHC and phosphine donors in those studies are joined via a methylene bridge, thus giving stable five-membered chelate structures. One may consider these NHCP-congeners **E** the *cis*-coordination analogues of a second generation Grubbs catalyst **B**. Notable differences between the highly active bisphosphine system **F1** and **G** are evident, such as the increasing of the chelate ring system from four-membered to a less

Received: March 6, 2015

DOI: 10.1021/acs.inorgchem.5b00513
Inorg. Chem. XXXX, XXX, XXX−XXX

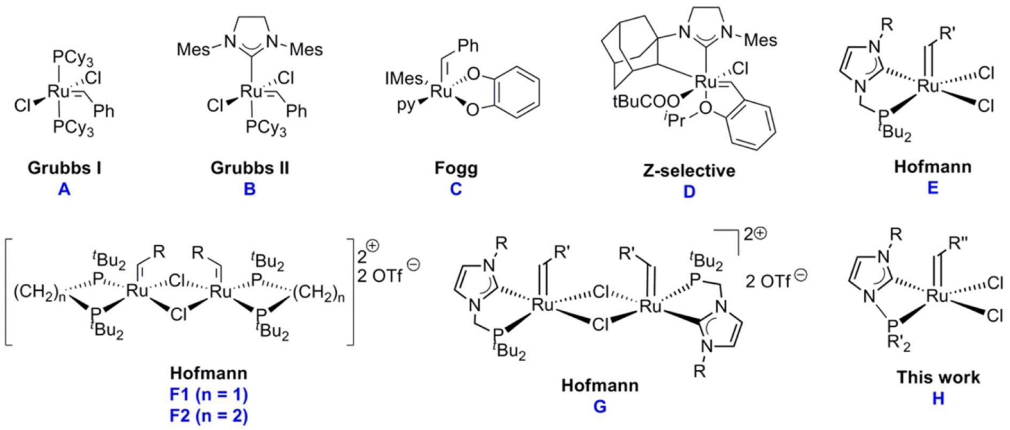

Figure 1. Selected olefin metathesis catalysts.

strained five-membered chelate ring and reduced steric bulk proximal to the metal center. Studies are currently underway into the evaluation of the properties of **G**, and the cationic versions of **E**, the direct NHCP analogues of **F2**. Consequently, it was an open question whether the preparation and evaluation of four-membered ruthenium NHC-phosphine complexes, such as neutral mononuclear **H**, may provide improvements in stability over bis-phosphine **F1** or of catalytic activity over NHC-phosphine complexes such as (**G**). For complexes of the type **H**, their four-membered chelate structures—if these species are accessible—may provide the possibility of strained chelate ring opening (hemilability) and generation of active Ru 14 VE intermediates which are widely believed to initiate the olefin coordination step in Grubbs second based olefin metathesis (vide infra).

The first synthesis of an NHCP ligand system for Ru-complexes of type **H** (R = C_2H_5, R′ = *t*Bu) with a direct nitrogen−phosphorus bond was achieved in 2007 by our group.[11a] Soon after in 2010 an elegant more general synthesis of such ligands was published by Marchenko et al., followed up by slight synthetic variations for a broader scope of ligands in 2012.[12b,c] These syntheses provided the opportunity to investigate their metal coordination chemistry. Our first communication into this area for Ru described the unexpected reaction between a ruthenium alkylidene and an NHCP ligand,[13] following investigations involving group 10 and 11 metals.[11,12c,14] While such NHCP ligands have a general tendency to act as bridging ligands between metal centers, this has only been observed for group 11 metals, and otherwise, the desired four-membered chelate structures have been found. Our previous report on the subject of N-phosphino functionalized NHC ligands included a considerable computational study into the behavior of a NHCP ligand and a ruthenium center. While the reader may refer to this publication for a full description of our results, one computational finding relevant to the present work is briefly described and presented in Scheme 1. Beginning with a five-coordinate Ru-NHCP alkylidene dichloride species, **X1**, we showed computationally that phosphine dissociation leading to **X2**, was a reasonably facile reaction, while carbene-C dissociation to **X5** was energetically prohibitive, as expected from the known chemistry of NHC vs phosphine ligands. Species **X2** can be considered comparable to the active 14 VE species of a second generation Grubbs type catalyst system. From species **X2** the catalytic cycle may proceed via olefin coordination, **X3**, and metallacyclobutane formation, **X4**, leading to catalytic olefin metathesis.

Scheme 1. Hemilabile Behavior of Ru-NHCP Complexes of Type H where R = Me and R′ = tBu

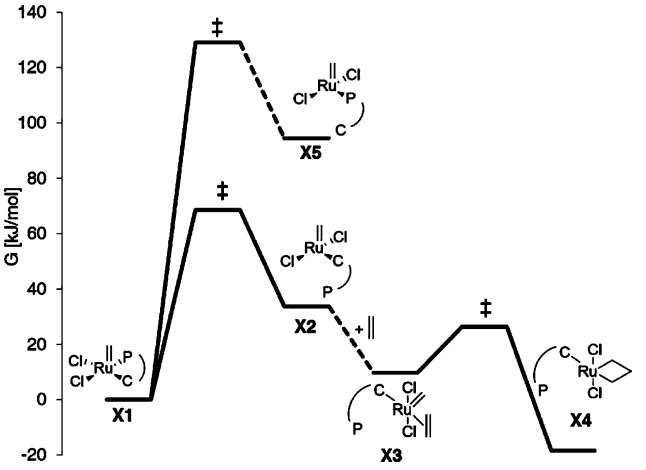

We report herein the synthesis of bidentate NHCP ligands of the form **2a−c**, a convenient entry into their ruthenium coordination chemistry and the preparation of the corresponding ruthenium alkylidene complexes. We describe the synthesis of a sufficiently reactive ruthenium precursor for the formation of these ruthenium alkylidenes from diazo reagents. Trimethylsilyl-alkylidene complexes are presented first, synthesized from the commercially available trimethylsilyldiazomethane, and their behavior with respect to catalysis is described. Furthermore, an example of a benzylidene complex has been prepared and is compared to its trimethylsily substituted congeners.

RESULTS AND DISCUSSION

Ligand Synthesis. Our research group and others have recently developed a simple, high yielding, and scalable synthesis of N-phosphino-functionalized N-heterocyclic carbene ligands (NHCPs). The NHCP salt precursor, **1a**, and its corresponding free NHCPs, **2a** and **2c**, have been previously described in the literature, while compounds **1b**, **1c**, and **2b** have been newly prepared during the course of this study, using slight modifications of reported procedures (Scheme 2). The newly prepared NHCP compounds showed a similar ease of synthesis with the exception of the *N*-*tert*-butyl-*N*′-di-*tert*-butyl-

DOI: 10.1021/acs.inorgchem.5b00513
Inorg. Chem. XXXX, XXX, XXX−XXX

Scheme 2. Synthesis of NHCP Salts and Free NHCP Ligands 2a−c[a]

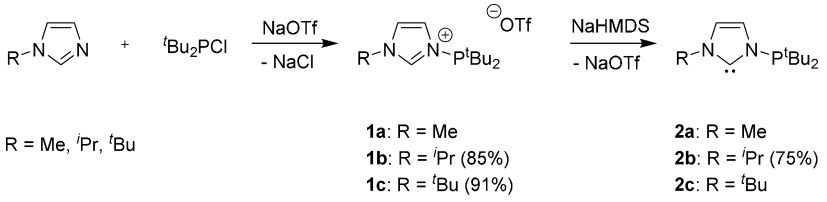

[a]Yields are given in brackets for newly prepared compounds.

phosphino-functionalized N-heterocyclic carbene **2c** (Scheme 2), which could be only isolated as a viscous oily compound which hampers complete purification. Subsequent reactivity, however, was always unaffected. As mentioned above, the C_2H_5-analogue of **2a** (R = Et instead of Me) was also accessible, although via a route different from the one shown in Scheme 2, as disclosed earlier,[12c] but this compound was not part of the present study.

The new NHCP salt **1b** has been fully characterized. The solid state molecular structure of **1b** displays the expected characteristics and is shown in Figure 2. Furthermore, NMR

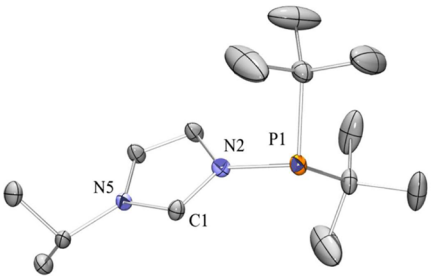

Figure 2. ORTEP plot of the cation of imidazolium triflate salt **1b**. Thermal ellipsoids are at the 30% probability level. Hydrogen atoms and the triflate anion are omitted for clarity. Selected bond length (Å): P1−N2 = 1.788(5) and angle (deg): C1−N2−P1 = 119.46 (44).

spectroscopy of **1b** had a ^{31}P NMR signal at 120.8 ppm, which, upon deprotonation, shifted upfield to 97.2 ppm as expected. The previously reported NHCP compounds used in this study otherwise match the literature characterization data.[12a] It was expected, outside of noninnocent behavior as we have previously described, that such NHCP ligands will form four-membered rings upon ruthenium coordination.[13]

NHCP Coordination. A high yielding synthetic entry into mononuclear 16 VE ruthenium dichloride chemistry using $Ru(PPh_3)_3Cl_2$ as a convenient starting point was developed. Mixing an equimolar solution of $Ru(PPh_3)_3Cl_2$ and **2a** in THF afforded **3a** in 86% isolated yield within 1 h at room temperature. The initial red-brown color of $Ru(PPh_3)_3Cl_2$ is quickly lost, and a deep purple solution is formed. The product precipitates from THF forming microcrystalline bulk material. Analysis of an NMR scale reaction shows the complete consumption of **2a** and the liberation of free PPh_3 via ^{31}P NMR spectroscopy. The reaction can be scaled up easily and can be run as efficiently on a multigram scale. Analysis of isolated **3a** displays two coupled doublets in the $^{31}P\{^1H\}$ NMR. A doublet at 104.3 ppm corresponds to the coordinated NHCP phosphorus fragment, while a doublet at 77.3 ppm corresponds to one remaining coordinated PPh_3. One coordinated PPh_3 is also implied by the ^1H NMR of **3a** relative to one coordinated NHCP ligand (**2a**). The molecular structure of **3a** was confirmed via single crystal X-ray crystallography (Figure 3). The structure of **3a** shows that it adopts a distorted square

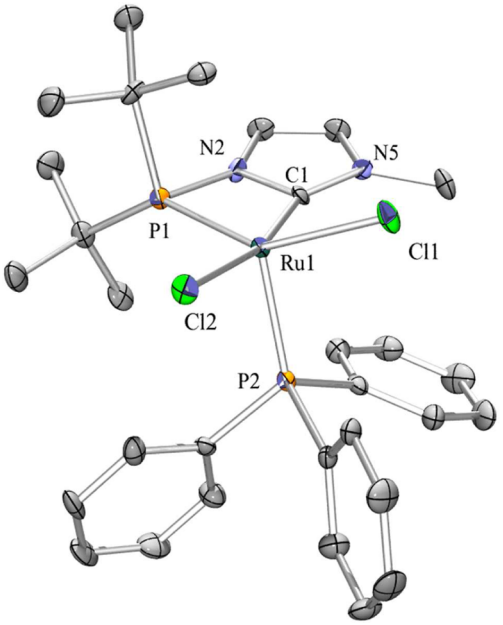

Figure 3. ORTEP plot of ruthenium complex **3a**. Thermal ellipsoids are at the 30% probability level. Hydrogen atoms are omitted for clarity. Selected bond lengths (Å) Ru1−C1 = 1.996(7); Ru1−P1 = 2.303(2); Ru1−P2 = 2.225(2); Ru1−Cl1 = 2.405(2); Ru1−Cl2 = 2.464(2); P1−N2 = 1.743(6) and angles (deg) P1−Ru1−C1 = 67.6(2); P1−N2−C1 = 100.3(4).

pyramidal geometry about the ruthenium center. The NHCP ligand coordinates via the expected four-membered chelate structure with two *trans*-disposed chlorides completing the base of the square pyramidal configuration. One coordinated PPh_3 forms the apex of the distorted square pyramid. The angles about the base sum to 355.3° showing the slight distortion. The NHCP-carbon−ruthenium bond distance was found to be 1.996(7) Å with a NHCP-phosphorus−ruthenium bond distance of 2.3032(19) Å. The Ru−Cl bond distances are 2.4636(18) Å and 2.4051(18) Å *trans* to carbon and phosphorus, respectively. The Ru−PPh_3 bond distance is 2.2247(19) Å. The Ru-NHCP bite angle was determined to be 67.6(2)°, which confirms the expected bidentate nature of our NHCP ligands.

Complexes **3b** and **3c** were prepared using a similar synthetic procedure as for **3a**. **3b** and **3c** were isolated in 79% and 56% yields, respectively. Changing the supporting NHCP ligand from R = Me to ^{i}Pr to ^{t}Bu systematically reduces the isolated yield due to the increased solubility and difficulty of PPh_3 separation. However, monitoring of the reaction via NMR

DOI: 10.1021/acs.inorgchem.5b00513
Inorg. Chem. XXXX, XXX, XXX−XXX

Scheme 3. Synthesis of 3a−c[a]

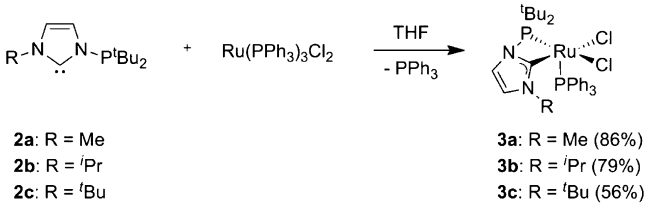

2a: R = Me
2b: R = ^{i}Pr
2c: R = ^{t}Bu

3a: R = Me (86%)
3b: R = ^{i}Pr (79%)
3c: R = ^{t}Bu (56%)

[a]Yields are given in brackets for newly prepared compounds.

spectroscopy shows similar conversions. **3b** displays two doublets in the $^{31}P\{^{1}H\}$ NMR spectrum, 108.9 and 77.7 ppm, indicative of a similar coordination mode about the ruthenium center as **3a**. The ^{1}H NMR spectrum shows a slight broadening of the aromatic proton signals attributed to the PPh_3 ligand. **3b** was characterized via single crystal X-ray diffraction (Figure 4, left) and reveals an analogous geometry as **3a**. The NHCP-carbene−ruthenium bond distance was found to be 2.024(4) Å, while the NHCP-phosphorus−ruthenium bond distance was found to be 2.3063(12) Å. A PPh_3 was again the apex of a slightly distorted square pyramid with a Ru−PPh_3 bond distance of 2.2199(12) Å. **3c** displays similar spectroscopic characteristics as **3a** and **3b** with one notable difference in its solution ^{1}H NMR. While the $^{31}P\{^{1}H\}$ NMR displays two doublets at 110.8 and 72.6 ppm, the ^{1}H NMR is significantly broadened especially for the aromatic protons of the PPh_3. This would suggest inhibited rotation about the Ru−PPh_3 bond. This observation is only significant for the most bulky Ru-NHCP complex **3c** (Figure 4, right). An NHCP-carbene−ruthenium bond distance of 2.048 Å, the average for two molecules in the asymmetric unit, and the NHCP-phosphorus−ruthenium bond of 2.280 Å, again the average for two molecules in the asymmetric unit, were not found to be significantly different for **3c** compared to those found in **3a** and **3b**. Furthermore, the Ru−PPh_3 bond distance found in **3c** is not significantly different from those distances found in **3a** and **3b**.

The synthesis of **3a**, **3b**, and **3c** stands in contrast to our attempts toward the synthesis of N-aryl-NHCP ruthenium complexes. We have previously reported that the reaction of $Ru(PPh_3)_3Cl_2$ with N-mesityl-NHCPs leads uncontrollably to an octahedral bis-chelation ruthenium *trans*-dichloride complex.[12c] It was clear that alternative synthetic pathways will thus be required to obtain the desired monochelation N-aryl-NHCP ruthenium complexes.

Synthetic Variations. Indeed, complexes **3a−c** provided a convenient entry into 16 VE Ru(II) coordination chemistry, although complexes **3a−c** proved to be substitutionally rather inert. Screening reactions of **3a−c** with trimethylsilyldiazomethane and phenyldiazomethane showed only small conversions to what could be considered the desired products **5a−c** and **6a−c** via ^{1}H and ^{31}P NMR spectroscopy. On the basis of these observations it was decided that a more labile ligand than PPh_3 would be desirable. Pyridine and substituted pyridines have been shown to be widely useful in transition metal catalysis as labile spectator ligands in a variety of applications, e.g., in catalytic olefin metathesis and in transition metal mediated hydrogenation, because they are more weakly bound to the metal center and thus ease ligand substitution.[3a,15]

Using complex **3a** as a test system in order to assess the efficacy of PPh_3-pyridine ligand exchange reactions and subsequent metal complex reactivity, we examined the role of pyridine, 2-methylpyridine (2-picoline), and 3-bromopyridine. These three examples should provide an electronic (3-bromopyridine), and a steric (2-methylpyridine) modification, in contrast to pyridine itself. The reaction of **3a** with neat pyridine showed an immediate color change from purple to orange and the precipitation of an orange solid. Examination of the crude reaction mixture, $\mathbf{4a_H}$, via ^{31}P NMR spectroscopy displayed no further $^{31}P\{^{1}H\}$ coupling, the presence of uncoordinated PPh_3, and several signals between 120 and 105 ppm, likely corresponding to a coordinated NHCP ligand in deuterated dichloromethane as solvent. Analysis of a purified sample of $\mathbf{4a_H}$ in deuterated CD_2Cl_2 showed four singlet signals in the ^{31}P NMR spectrum. The ^{1}H NMR also showed four distinct sets of signals. The NMR spectra of an identical sample

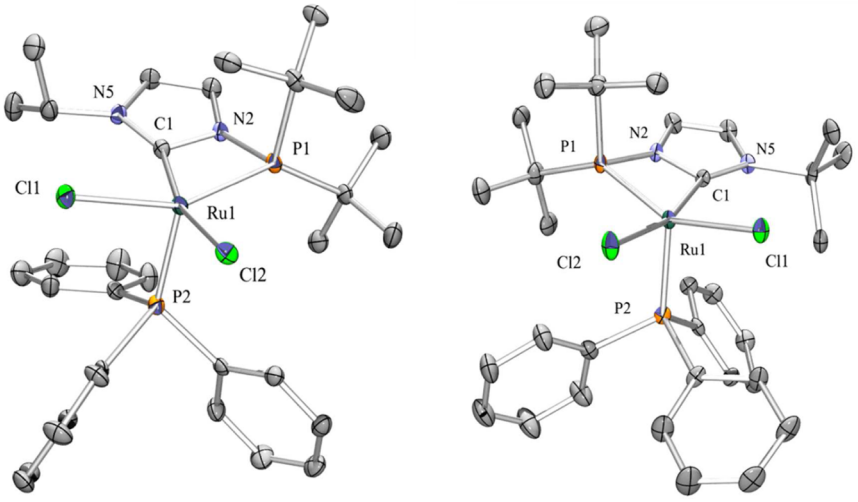

Figure 4. ORTEP plot of ruthenium complexes **3b** and **3c**. Thermal ellipsoids are at the 30% probability level. Hydrogen atoms are omitted for clarity. Selected **3b** bond lengths Ru1−C1 = 2.024(4); Ru1−P1 = 2.306(1); Ru1−P2 = 2.220(1); Ru1−Cl1 = 2.416(1); Ru1−Cl2 = 2.469(1); P1−N2 = 1.749(3) and angles (deg) P1−Ru1−C1 = 67.2(1); P1−N2−C1 = 99.6(3) **3c** bond lengths Ru1−C1 = 2.04(1); Ru1−P1 = 2.281(4); Ru1−P2 = 2.227(4); Ru1−Cl1 = 2.419(3); Ru1−Cl2 = 2.445(4); P1−N2 = 1.72(1) and angles (deg) P1−Ru1−C1 = 67.7(4); P1−N2−C1 = 101.9(8).

DOI: 10.1021/acs.inorgchem.5b00513
Inorg. Chem. XXXX, XXX, XXX−XXX

Scheme 4. Synthesis of Ruthenium Pyridine Complexes 4a−c[a]

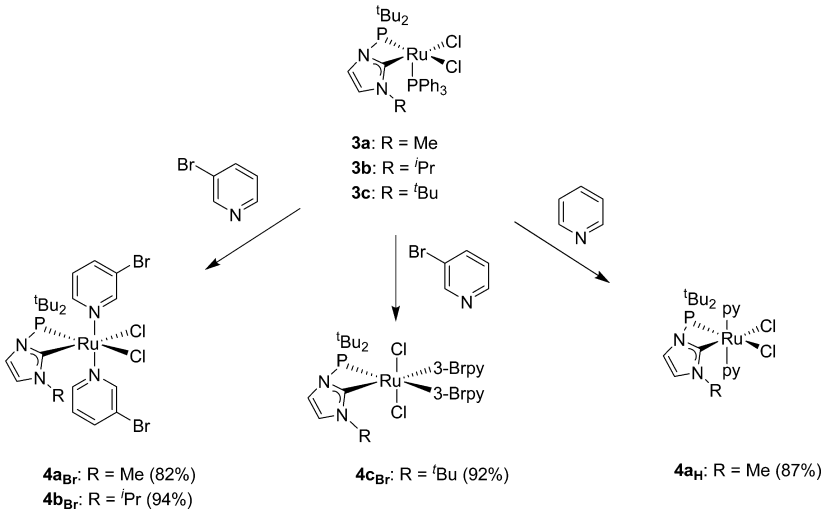

[a]Yields are given in brackets for newly prepared compounds.

recorded in deuterated pyridine, however, displayed far fewer signals. In deuterated pyridine only two signals are visible in the $^{31}P\{^{1}H\}$ NMR spectrum at 113.9 and 107.5 ppm. Furthermore, ^{1}H NMR spectroscopy revealed proton signals which corresponded to only two compounds. For example, two signals at 4.26 and 4.68 ppm indicated two different N−CH3 groups. From this we conclude that different mixtures of isomers are formed, the relative concentration of which is strongly dependent on the solvent. In deuterated pyridine two isomers are present in an approximately 70:30 ratio based on ^{1}H NMR. One may imagine several isomers of a complex such as $\mathbf{4a_H}$ particularly if in noncoordinating solvents one equivalent of pyridine is not coordinated to the ruthenium center. Our observations support that in dichloromethane the complex is likely in equilibrium with a species missing one pyridine by dissociation, or at least with one pyridine not strongly bound, and that the addition of pyridine forces coordinative saturation of the metal center, thus reducing the number of isomers. The solid state structure of $\mathbf{4a_H}$ which was unambiguously assigned using single crystal X-ray diffraction, and elemental analysis further supports our structural assignment. The diffraction study revealed an octahedral 18 VE ruthenium species (Figure 5). The structure showed two *trans*-disposed pyridines, a bidentate equatorial NHCP ligand, and two *cis*-chlorides with the pyridine ligands showing slight bending away from the NHCP ligand. The NHCP-carbene ruthenium bond length was determined to be 2.009(3) Å, the NHCP-phosphorus ruthenium bond length was found to be 2.3308(7) Å, and the Ru−Cl bond lengths were determined to be 2.5200(7) Å and 2.4673(7) Å *trans* to the carbene and phosphorus, respectively. The C−Ru−P bite angle of the NHCP ligand was determined to be 66.16(7)°. These values represent only slight deviations from the bond lengths and bite angle found in **3a**. The ruthenium-pyridine Ru−N distances are 2.099(2) Å and 2.132(2) Å, which are similar to those found in analogous ruthenium complexes, such as $SIMesRuCl_2py_2$.[16] We carried out screening reactions with pyridine complex $\mathbf{4a_H}$ to form the desired complexes **5a** and **6a**. In test reactions with trimethylsilyldiazomethane and phenyldiazomethane only a marginal increase in reactivity was observed over **3a**; furthermore, $\mathbf{4a_H}$ was observed to be relatively insoluble in

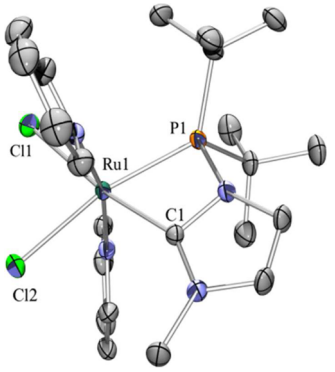

Figure 5. ORTEP plot of ruthenium complex $\mathbf{4a_H}$. Thermal ellipsoids are at the 30% probability level. Hydrogen atoms are omitted for clarity. Selected bond lengths (Å) Ru1−C1 = 2.009(3); Ru1−P1 = 2.3308(7); Ru1−N21 = 2.099(2); Ru1−N31 = 2.132(2); Ru1−Cl1 = 2.5200(7); Ru1−Cl2 = 2.4673(7); P1−N2 = 1.742(2) and angles (deg) P1−Ru1−C1 = 66.16(7); P1−N2−C1 = 99.1(2).

common solvents. The reactions of $\mathbf{4a_H}$ with diazo reagents consistently resulted in the synthesis of some so far unidentified ruthenium products and substantial amounts of remaining starting material ($\mathbf{4a_H}$). Considering the observation that $\mathbf{4a_H}$ had little improvement in terms of reactivity we did not carry out further studies into the behavior of $\mathbf{4a_H}$.

The mixing of **3a** with 2-methylpyridine (2-picoline), either neat or using dichloromethane as a solvent, did not result in an immediate reaction. In fact, as opposed to pyridine, **3a** does not dissolve in 2-methylpyridine and dichloromethane is required to solubilize **3a**. Prolonged heating and mixing of a mixture of **3a** and 2-methylpyridine also resulted in limited conversion, no new isolable products, and eventually to the production of ruthenium black. Presumably, *ortho*-substituted pyridines are too bulky to coordinate efficiently to **3a** and to replace PPh_3.

In an effort to assess the electronic affects of electron withdrawing substituents on pyridine, we explored the formation of ruthenium 3-bromopyridine complexes. The mixing of **3a** with 3-bromopyridine resulted in an immediate color change from purple to orange, analogous to what was observed during the synthesis of $\mathbf{4a_H}$. The NMR of an isolated sample of $\mathbf{4a_{Br}}$ once again revealed a complex spectrum. This

DOI: 10.1021/acs.inorgchem.5b00513
Inorg. Chem. XXXX, XXX, XXX−XXX

observation is not entirely surprising given the expected increased lability of the 3-bromopyridine ligands relative to pyridine. The molecular structure was confirmed by single crystal X-ray diffraction. $\mathbf{4a_{Br}}$ displayed a distorted octahedral geometry. The molecular structure (Figure 6) was similar to

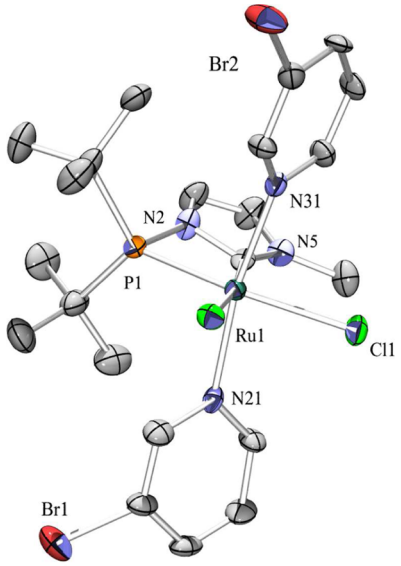

Figure 6. ORTEP plot of ruthenium complex $\mathbf{4a_{Br}}$. Thermal ellipsoids are at the 30% probability level. Hydrogen atoms are omitted for clarity. Selected bond lengths: Ru1−C1 = 1.99(1); Ru1−P1 = 2.347(3); Ru1−N21 = 2.087(8); Ru1−N31 = 2.127(8); Ru1−Cl1 = 2.471(3); Ru1−Cl2 = 2.526(3); P1−N2 = 1.738(9) and angles (deg) P1−Ru1−C1 = 66.4(3); P1−N2−C1 = 99.8(7).

that found for $\mathbf{4a_H}$. The NHCP ligand is situated in a plane with the *cis*-positioned chloride ligands. Two *trans*-pyridines complete the octahedron. The NHCP-carbene−ruthenium bond distance is 1.990(11) Å, the NHCP-phosphorus−ruthenium bond distance was determined to be 2.347(3) Å, and the Ru−Cl bond distances were found to be 2.526(2) Å and 2.472(2) Å *trans* to the carbene and phosphine, respectively. The NHCP-Ru bite angle amounts to 66.4(3)°, and the ruthenium 3-bromopyridine Ru−N bond distances were found to be 2.087(8) Å and 2.128(8) Å. Comparing the experiential ruthenium−pyridine bond distances between $\mathbf{4a_H}$ and $\mathbf{4a_{Br}}$ shows that the electron withdrawing 3-bromopyridine has little to no effect on the ruthenium−pyridine bond distances. Complex $\mathbf{4a_{Br}}$ shows improved solubility over complex $\mathbf{4a_H}$.

We also investigated the synthesis of complexes $\mathbf{4b_{Br}}$ and $\mathbf{4c_{Br}}$, more bulky analogues of $\mathbf{4a_{Br}}$. Dissolving **3b** in a minimum amount of 3-bromopyridine resulted in a quick reaction to form a new orange complex $\mathbf{4b_{Br}}$. However, so far it was not possible to obtain suitable single crystals for a solid state structure determination; therefore, we cannot definitively assign the molecular structure, but NMR spectroscopy suggests a similar coordination sphere as $\mathbf{4a_{Br}}$. Finally, dissolving **3c** in a minimum amount of 3-bromopyridine also yielded a new orange complex, $\mathbf{4c_{Br}}$. The molecular geometry of this species could be again assigned via single crystal X-ray diffraction to reveal a nearly ideal octahedral geometry. Remarkably, the structure of $\mathbf{4c_{Br}}$ in the solid state (Figure 7) differs compared to that found for $\mathbf{4b_{Br}}$. $\mathbf{4c_{Br}}$ displays a plane consisting of a NHCP ligand and two 3-bromopyridine ligands. Two chloride

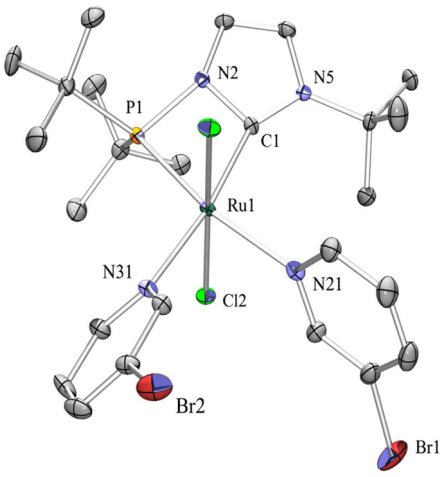

Figure 7. ORTEP plot of ruthenium complex $\mathbf{4c_{Br}}$. Thermal ellipsoids are at the 30% probability level. Hydrogen atoms are omitted for clarity. Selected bond lengths: Ru1−C1 = 2.060(4); Ru1−P1 = 2.296(1); Ru1−N21 = 2.257(4); Ru1−N31 = 2.169(3); Ru1−Cl1 = 2.432(1); Ru1−Cl2 = 2.417(1); P1−N2 = 1.740(4) and angles (deg) P1−Ru1−C1 = 66.4(1); P1−N2−C1 = 99.5(3).

ligands complete the axial coordination sites of the octahedral framework. An NHCP-carbene−ruthenium bond distance of 2.060(4) Å was found, with NHCP-phosphorus−ruthenium and the two ruthenium-chloride bond distances of 2.296(1) Å, 2.417(1) Å, and 2.433(1) Å, respectively. In this case, the ruthenium 3-bromopyridine Ru−N bond distances of 2.169(3) Å and 2.257(4) Å *trans* to the NHCP carbene and phosphorus correspondingly were found. These data show that there is a considerable lengthening of the ruthenium−pyridine bonds in $\mathbf{4c_{Br}}$ in comparison to that found in $\mathbf{4a_{Br}}$. The NMR spectra of both $\mathbf{4b_{Br}}$ and $\mathbf{4c_{Br}}$ are equally complex to that observed for $\mathbf{4a_{Br}}$.

Synthesis of Ruthenium Alkylidene Complexes. Following a similar synthetic procedure as that used in the initial synthesis of Grubbs precatalysts, we employed derivatized diazomethane reagents, specifically trimethylsilyldiazomethane and phenyldiazomethane, as synthetic precursors for Ru alkylidene species. Initially we explored the synthesis of ruthenium complexes bearing trimethylsilyl alkylidene functionalities derived from commercially available trimethylsilyldiazomethane for synthetic ease and efficiency. While less commonly used as an olefin metathesis initiator than benzylidene- and indenylidene-based complexes, there are reports of the effective use of trimethylsilyl alkylidenes in catalytic olefin metathesis.[17] Complexes $\mathbf{4a_{Br}}$, $\mathbf{4b_{Br}}$, and $\mathbf{4c_{Br}}$ all showed improved reactivity with diazomethane reagents in small scale reactivity screening when compared to the previously prepared complexes in this study; therefore, complexes $\mathbf{4a_{Br}}$, $\mathbf{4b_{Br}}$, and $\mathbf{4c_{Br}}$ were more closely examined as precursors to ruthenium-alkylidene complexes.

A solution of $\mathbf{4a_{Br}}$ in dichloromethane cooled to −40 °C was reacted with a commercial 2 M solution of trimethylsilyldiazomethane (in hexanes) with warming to room temperature. Nearing room temperature the solution began to bubble with a slow change of color from purple to green. Isolating the green product, **5a**, from THF and analysis via NMR spectroscopy revealed the formation of one new complex. Most indicatively, a doublet at 18.61 ppm in the proton NMR suggests the formation of a ruthenium alkylidene bond as desired.

DOI: 10.1021/acs.inorgchem.5b00513
Inorg. Chem. XXXX, XXX, XXX−XXX

Scheme 5. Synthesis of Ruthenium Trimethylsilyl-Alkylidene Complexes 5a−c and 6c[a]

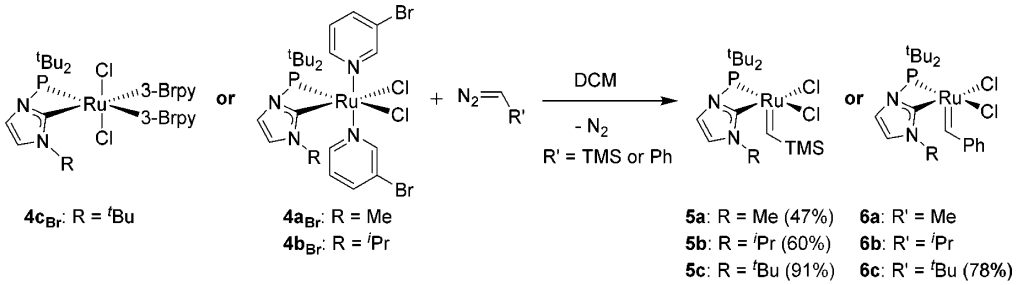

[a]Yields are given in brackets for newly prepared compounds.

Furthermore, a new TMS signal is visible at 0.38 ppm, one signal for the NHCP methyl substituent is observed at 3.52 ppm, two signals for the imidazole backbone, and two dissimilar ^{t}Bu signals for the NHCP ligand were present as expected. The ^{31}P NMR showed one singlet for the di-*tert*-butylphosphine fragment of the NHCP chelate ligand. Crystals suitable for a single crystal X-ray diffraction study allowed for the unambiguous determination of the molecular structure and revealed a distorted square pyramidal arrangement (Figure 8).

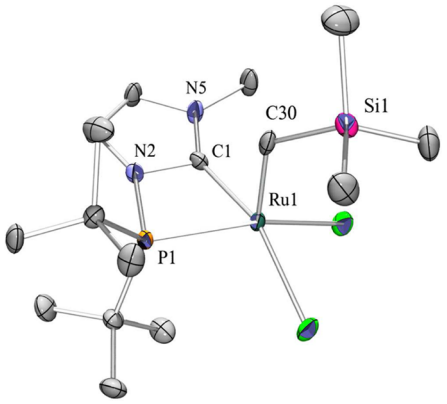

Figure 8. ORTEP plot of ruthenium complex **5a**. Thermal ellipsoids are at the 30% probability level. Hydrogen atoms are omitted for clarity. Selected bond lengths: Ru1−C1 = 1.987(6); Ru1−P1 = 2.288(2); Ru1−C30 = 1.829(6); Ru1−Cl1 = 2.438(1); Ru1−Cl2 = 2.395(2); P1−N2 = 1.737(4) and angles (deg) P1−Ru1−C1 = 67.2(2); P1−N2−C1 = 99.0(3).

The NHCP ligand along with two chloride ligands forms the base of the square pyramidal structure with the alkylidene group positioned as the apex. An NHCP-carbene−ruthenium bond distance of 1.987(6) Å was determined, the NHCP-phosphorus−ruthenium bond distance is 2.288(2) Å, and the ruthenium chloride bonds distances were found to be 2.438(1) Å and 2.395(2) Å *trans* to the carbene and phosphorus, respectively. The NHCP bite angle amounts to 67.2(2)°, while the sum of the angles at the metal in the base of the square pyramid is 352.7°, showing a slight distortion of the complex. The ruthenium alkylidene bond distance of 1.829(6) Å is one of only two known structurally characterized examples of ruthenium TMS-alkylidene complexes, the other example having the TMS-alkylidene unit at the apex of a ruthenium porphyin complex.[18] Regardless, the ruthenium alkylidene bond distance of 1.829(6) Å is very similar to the ruthenium alkylidene bond distance of 1.839(3) Å found in the second generation Grubbs catalyst.[19]

As in the case of $\mathbf{4a_{Br}}$ we explored the preparation of ruthenium TMS-alkylidene complexes using $\mathbf{4b_{Br}}$ and $\mathbf{4c_{Br}}$. The reaction of $\mathbf{4b_{Br}}$ with trimethylsilyldiazomethane, with conditions similar to those used to prepare **5a**, yielded a new green complex (**5b**). Analysis of the sample with NMR once again showed the formation of a new alkylidene signal in the ^{1}H NMR at 18.56 ppm. A single crystal analyzed via X-ray crystallography revealed a structure similar to that found for **5a**. Similar metrical parameters as in **5a** characterize the molecular structure of **5b** (Figure 9). The ruthenium−alkylidene bond

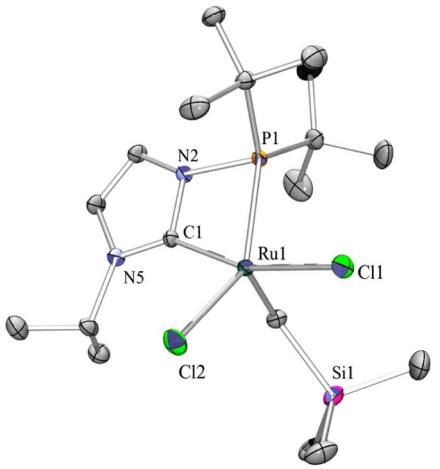

Figure 9. ORTEP plot of ruthenium complex **5b**. Thermal ellipsoids are at the 30% probability level. Hydrogen atoms are omitted for clarity. Selected bond lengths: Ru1−C1 = 2.010(2); Ru1−P1 = 2.2962(4); Ru1−C30 = 1.829(2); Ru1−Cl1 = 2.4400(5); Ru1−Cl2 = 2.3773(5); P1−N2 = 1.732(2) and angles (deg) P1−Ru1−C1 = 66.81(5); P1−N2−C1 = 99.7(1).

length is 1.829(2) Å, while the NHCP bite angle was found as 66.81(5)°. The distortion of the square pyramidal structure was similar to the case of **5b**, with the sum of the angles around the basal Ru-position of the square pyramid equal to 352.63°.

While we were unable to obtain a molecular structure of **5c**, the NMR data of **5c** were fully consistent with a molecular geometry as those found in **5a** and **5b**. The ^{1}H NMR revealed a new alkylidene signal at 18.98 ppm, dissymmetric ^{t}Bu signals for the di-*tert*-butylphosphino fragment, and one new TMS signal for the trimethylsilylalkylidene.

The synthesis of **5c** appeared to be the most straightforward, high yielding, and scalable route to a ruthenium TMS-alkylidene and therefore was used first to synthesize Ru-NHCP benzylidene complexes. The synthesis of **5c** could be undertaken on the gram scale, while the synthesis of **5a** and **5b**

DOI: 10.1021/acs.inorgchem.5b00513
Inorg. Chem. XXXX, XXX, XXX−XXX

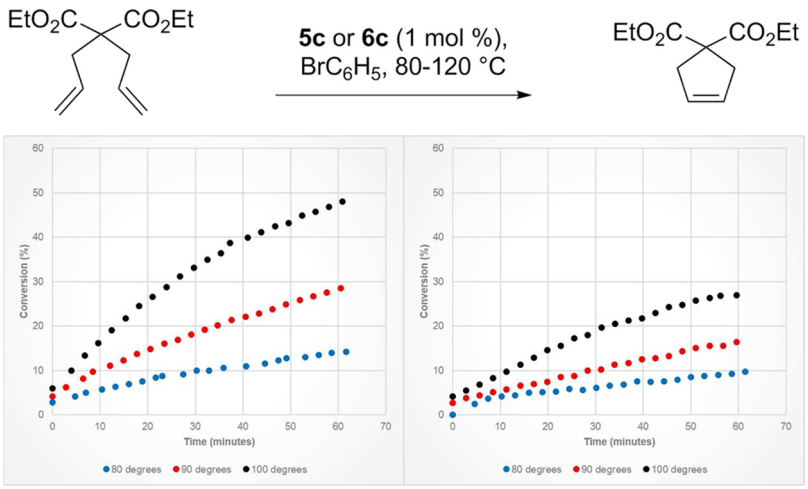

Figure 10. Performance of **6c** (left) and **5c** (right) in the RCM of diethyl diallylmalonate. Condition (0.1 M, cat. 1 mol %, bromobenzene 0.75 mL). Reaction monitored every 3 min using high temperature NMR.

did not scale well beyond the 200 mg scale (without further optimization). The mixing of $\mathbf{4c_{Br}}$ and phenyldiazomethane in a dichloromethane solution cooled to −40 °C resulted in the vigorous bubbling of the reaction mixture and in a color change from orange to deep green. Using procedures similar to those used in the synthesis of $\mathbf{4c_{Br}}$ yielded a new product **6c**. NMR analysis showed the clean formation of a single new species. It displayed a new ^{1}H NMR resonance at 15.77 ppm typical for a ruthenium-alkylidene fragment. This signal differs significantly from that observed in **5c**, 3.21 ppm upfield of that observed for $\mathbf{4c_{Br}}$. The ^{31}P NMR signal for **6c** was detected at 130 ppm compared to a ^{31}P signal at 137 ppm for **5c**.

We have thus far been unable to prepare the complexes **6a** and **6b**. Following both identical as well as modified procedures varying the temperature, solvent, and reaction time screening or modifying the workup strategies compared to those employed in the synthesis of **5a**−**c** and **6c** resulted in mixtures of unidentified products. Importantly, no new ^{1}H alkylidene signals were observed. The reason for the contrasting reactivity of **5c** versus **5a** and **5b** is elusive at this point. Two notable observations are that **5c** is significantly more soluble than the poorly soluble complexes **5a** and **5b**. Furthermore, the solid state structure of **5c** showed the pyridine ligands in the plane of the NHCP ligand, while the solid state structure of **5a** showed the pyridine ligands in the apical positions of the octahedral structure.

Screening of NHCP Ruthenium Alkylidene Complexes in Catalysis. As mentioned above, the motivation to synthesize Ru alkylidene complexes like **6a**−**c** was based upon their similarity to Grubbs II precatalysts. Contrasting those, our systems contain a chelate-enforced *cis*-coordination mode of an NHC carbon and a phosphine donor as parts of a presumably strained four-membered Ru−P−N−C chelate-ring, which may open a pathway from a pentacoordinate, square pyramidal 16 VE precatalysts like **6a**−**c** to tetracoordinate, catalytically active 14 VE species via Ru−P dissociation. These four-coordinate, highly reactive intermediates created from, e.g., **6a**−**c**, would obviously be structurally identical to the active species formed from Grubbs II precatalysts by phosphine (e.g., PCy_3) dissociation. As we knew from preliminary density functional theory (DFT) calculations on model systems and from established chemistry that the alternative Ru−C bond dissociation of the NHCP chelate rings should not compete with P-dissociation, we had set out to make appropriate Ru-NHCP-alkylidenes as described.

To compare the catalytic efficacy of our Ru-NHCP complexes, we focused our efforts on complexes **5c** and **6c** due to easy access to larger amounts of these complexes. This choice also was expected to allow an evaluation of the influence of the alkylidene functionality and its impact on catalysis. To benchmark the catalytic potential of **5c** and **6c**, we investigated the ring closing metathesis (RCM) of diethyl diallylmalonate, based on the standard catalytic conditions suggested by Grubbs, and the ring opening metathesis polymerization (ROMP)/ring expansion (RE) of cyclooctene, a reaction in which we have a long-standing interest.[20]

Both complexes **5c** and **6c** did not effect the RCM catalysis of diethyl diallylmalonate at room temperature. Using variable temperature NMR to investigate this RCM test reaction, we found that some catalysis is observed beginning at 60 °C, whereas at 80 °C we were able to observe appreciable catalytic activity. For the high temperature NMR studies bromobenzene-d_5 was used as the deuterated reaction solvent due to its convenient temperature range and the good solubility of the ruthenium complexes. The RCM reaction was monitored at 80, 90, and 100 °C using high temperature NMR and measuring spectra approximately every 3 min. Figure 10 shows that over the course of 1 h the conversion is 15%, 27%, and 48% at 80, 90, and 100 °C, respectively for **6c** and 10%, 16%, and 27% at 80, 90, and 100 °C, respectively, for **5c**. The rate of conversion over the course of 1 h is approximately linear with a slight fall off of activity over time at 100 °C, which may be attributed to catalyst decomposition. This pattern holds such that at 120 °C the RCM of diethyl diallylmalonate is 94% complete within the span of 1 h, catalyzed by **6c**. These findings demonstrate that our catalyst system is behaving in a latent fashion. Actually, few olefin metathesis systems have been shown to behave this way. One notable recent example is a report by Cazin and co-workers.[21] Furthermore, these data demonstrate that while a TMS substituted alkylidene is less competent at the RCM of diethyl diallylmalonate than a phenyl substituted alkylidene, it can still provide access to an active catalyst system via a commercially available alkylidene precursor.

The ROMP/RE of *cis*-cyclooctene is a reaction with significant industrial interest.[20b,22] It is used to produce an industrially important polymer in the polymer blending field.[23]

DOI: 10.1021/acs.inorgchem.5b00513
Inorg. Chem. XXXX, XXX, XXX−XXX

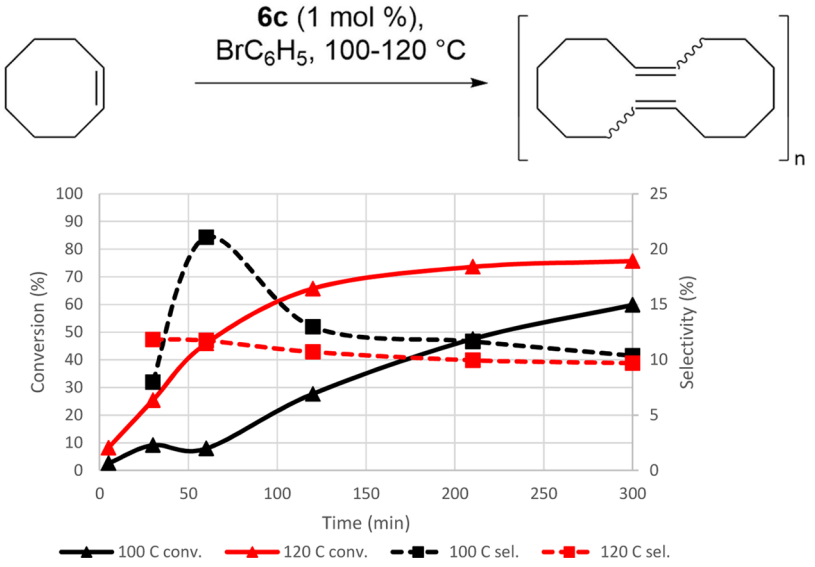

Figure 11. ROMP/RE of *cis*-cyclooctene. Solid line: conversion of *cis*-cyclooctene with respect to time. Dashed line: selectivity for 1,9-cyclohexadecadiene with respect to time. Yield and selectivity determined by GC. 1 mol % catalyst loading, 0.1 M concentration of cyclooctene in bromobenzene.

The controlled RE of cyclooctene, on the other hand, represents an entry point into the production of high value macrocyclic olefins, attractive precursors in the fragrance and flavor industry. A key example is the dimerization of cyclooctene to 1,9-cyclohexadecadiene. A substantial challenge is the controlled dimerization avoiding subsequent telomerisation and/or polymerization. The current heterogeneous process for the formation of 1,9-cyclohexadecadiene produces significant amounts of byproducts, and selective homogeneous alternatives would be advantageous. It has been noted that dissymmetric ligands, such as those reported herein, may be important in the improvement of the desired C16-selectivity.[20a]

Similar to our observations with the RCM of diethyl diallylmalonate, the ROMP/RE of cyclooctene also required elevated temperatures. Bromobenzene was again utilized as the solvent because of its ability to solubilize the catalyst and its high boiling point. Running the ROMP/RE of cyclooctene with catalyst **6c** in Teflon-sealed reaction vessels, sampling revealed the reaction profile shown in Figure 11. At 100 °C over the course of 5 h 60% conversion was obtained, while at 120 °C a maximum conversion of 75% was obtained after 4 h. These observations also demonstrate that our catalyst system **6c** behaves in a latent fashion. Furthermore, at these conditions we achieve a peak selectivity of 21% for 1,9-cyclohexadecadiene at 100 °C with decreasing selectivity over time. While the selectivity is lower than one of our previously reported dissymmetric NHC systems, this compares favorably with respect to heterogeneous Re_2O7, with a selectivity of 6% at 70% conversion, and with heterogenized Grubbs type systems, which typically display conversions in the range of 20% under flow conditions.[20b] Upon completion of the reaction, removal of the solvent, and analysis of the resulting material by GPC analysis, we found that all samples were composed of a broad mixture of cyclooctene oligomers/polymers. Relevant polymer data are presented in Table 1 showing broad PDIs, very low M_n and M_w values ranging from approximately 2000−43000 g/mol.

Table 1. Data for the Polymer Obtained by Polymerization of *cis*-Cyclooctene with 6c

temp [°C]	M_n [g/mol]	M_w [g/mol]	PDI
100	714	**42.700**	59.8
120	425	**3.460**	8.1

Conclusions. Herein we have described an entry into square pyramidal 16 VE ruthenium alkylidene complexes via appropriate precursor compounds, using N-phosphino-functionalized NHC ligands (NHCP) forming four-membered chelate structures, and preliminary catalytic screening of some of these species is reported. Ruthenium NHCP dichloride PPh3 complexes, prepared in high yielding syntheses, which can be easily scaled up, formed the basis for this novel ruthenium coordination chemistry. From these complexes the successful synthesis of the desired ruthenium alkylidene complexes has been demonstrated. Ruthenium NHCP complexes have been shown to catalyze both the ring closing metathesis of diethyl diallylmalonate and the metathesis ring expansion of *cis*-cyclooctene. The new ruthenium-NHCP-alkylidene complexes provide a second generation of the initial bis-phosphine olefin metathesis catalysts initially reported in 1999 by Hofmann and co-workers.[11b] Ongoing efforts in our laboratory are directed toward extending the structural manifold of this family of four-membered chelating (NHCP)Ru-alkylidenes by synthesis, guided by further DFT studies, toward more extensive catalyst screening, understanding Ru-NHCP catalytic activity, and subsequent catalyst optimization. The results will be presented in due course.

General Considerations. All manipulations were carried out under an atmosphere of dry argon using standard Schlenk techniques or in an MBraun glovebox. Solvents were either purchased dry from Aldrich or dispensed from an MBraun SPS-800 solvent system. Solvents were stored over either sodium ingots or molecular sieves (4 Å). Solvents were degassed either via 3-freeze−pump−thaw cycles or sparging with argon for 30 min. Previously reported phosphorylated NHC salts, their corresponding free NHCs were prepared according to literature procedures.[12a,24] All other solvents and reagents where purchased from Aldrich or ABCR chemicals. The cyclooctene was distilled from sodium prior to use, and the diethyl diallyl

DOI: 10.1021/acs.inorgchem.5b00513
Inorg. Chem. XXXX, XXX, XXX−XXX

malonte was used as received. NMR spectra were recorded using a Bruker 200 or a Bruker 600 spectrometer. Chemical shifts are given in ppm referenced to solvent (^{1}H, ^{13}C) and relative to 85% H_3PO_4 for ^{31}P NMR. Abbreviations used are s = singlet, d = doublet, sept = septet, br = broad. *J*-coupling constants are reported in Hertz (Hz). Elemental analyses were performed by the "Mikroanalytisches Laboratorium der Chemischen Institute der Universität Heidelberg". Gas chromatography was performed on an Agilent 6890N modular GC base equipped with a split-mode capillary injection system and a flame ionization detector using a BGB-5 capillary column (BGB Analytik Vertrieb 20530-025; 30 m × 0.25 mm; He flow 1.0 mL/min, program: initial 50 °C for 5 min, ramp 10 °C/min, 300 °C for 15 min, ramp 10 °C/min, 320 °C for 8 min). Starting materials and products had following retention times: cyclooctene (t_R = 10.8 min), dodecane (t_R = 17.7 min), bromobenzene (t_R = 12.4 min), 1,9-cyclohexadecadiene (t_R = 25.8 min), and 1,9,17-cyclotricosatriene (t_R = 34.5 min). The response correction is detailed in the Supporting Information.

GPC analysis was performed by BASF SE. The GPC was calibrated using polystyrene standards in the range of *M* = 580 bis M 6 870 000. The particulars are as follows: elution solvent THF, temperature of 35 °C, flow rate of 1 mL/min, injection volume of 100 μL, and a concentration of 2 mg/mL. The detector used was a DRI HP 1100 UV Agilent 1100 MWD [254 nm].

For the X-ray diffraction studies data sets were collected on a Bruker APEX-II Quazar CCD diffractometer with Mo Kα radiation (λ = 0.71073 Å). Intensities were corrected for Lorentz and polarization effects, an empirical absorption correction was applied using SADABS[1] based on the Laue symmetry of the reciprocal space. Structure solved by direct methods and refined against F^2 with a Full-matrix least-squares algorithm using the SHELXTL (Version 2008/4 or 2013/3) software package.[25]

CCDC 1045646 (**1b**), 1045647 (**3a**), 1045648 (**3b**) 1045649 (**3c**), 1045650 (**4aH**), 1045651 (**4aBr**) 1045652 (**4cBr**), 1045653 (**5a**), and 1045654 (**5b**) contain the supplementary crystallographic data for this paper. These data can be obtained free of charge from The Cambridge Crystallographic Data Centre via www.ccdc.cam.ac.uk/data_request/cif.

Catalysis. The ring closing metathesis reactions were performed in line with the protocols described by Grubbs and co-workers. An example procedure is as follows: A stock solution of catalyst **6c** was prepared. **6c** (10 mg, 0.0189 mmol) was dissolved in CD_2Cl_2-d_2 (1 mL). 50 μL of this solution was added to an NMR along with bromobenzene-d_5 (0.75 mL) and diethyl diallylmalonate (23 μL, 0.094 mmol). The NMR tube was immediately inserted into the NMR spectrometer prewarmed to the desired temperature. The displayed NMR temperature was correlated to internal temperature using ethylene glycol in accordance to the procedures described by Bruker Instruments. For example, for a catalytic run at 80 °C the spectrometer was set to 74 °C.

The catalytic ring expansion of *cis*-cyclooctene was performed as in previous work in the area by Limbach and co-workers.[20a] An example procedure is as follows: A stock solution of catalyst **6c** was prepared. **6c** (10 mg, 0.0189 mmol) was dissolved in bromobenzene (10 mL). Five milliliters of the catalyst solution was added to a Teflon sealed reaction vessel followed by addition bromobenzene (5 mL), *cis*-cyclooctene (110 mg, 1 mmol), and dodecane (internal standard, 170 mg) for a total substrate concentration of 0.1 M. The Teflon sealed vessel was heated to 100 °C and samples taken at 5 min, 30 min, 1 and 2 h under a stream of Argon. The aliquot was filtered through a small amount of silica gel and analyzed via GC.

Selectivity was defined as follows: selectivity in product i. (Si) = (number of mole of cyclooctene converted in product (i)/(total number of cyclooctene converted).

*Synthesis of N-Isopropyl-N′-di(tert-butyl)phosphino-imidazolium Triflate (**1b**).* To a solution of *N*-isopropylimidazole (7.71 g, 70 mmol) and CF_3OSO_2Na (12.65 g, 73.5 mmol) in THF (75 mL) was added at −10 °C di(*tert*-butyl)-chlorophosphine (13.28 g, 73.5 mmol) dissolved in THF (50 mL). The reaction mixture was allowed to warm to room temperature and stirred for 24 h. The solvent was removed *in vacuo*, the solid residue was extracted in CH_2Cl_2 (100 mL), the insoluble solid was filtered off, washed with CH_2Cl_2 (3 × 10 mL), and the filtrate was concentrated *in vacuo* until crystal started to form then cooled to −40 °C to yield colorless crystals to give **1b** (24.06 g, 85%). ^{1}H NMR (CD_2Cl_2): 8.98 (s, ^{1}H, NC*H*N), 7.67 (s, ^{1}H, $C_{imidazole}$), 7.56 (s, ^{1}H, $C_{imidazole}$), 4.94 (sept, *J* = 6.7 Hz, 1H, C*H*(CH_3)$_3$), 1.58 (d, *J* = 6.7 Hz, 6H, CH(C*H*$_3$)$_3$), 1.25 (d, *J* = 13.6 Hz, 18H, P(C(C*H*$_3$)$_3$)$_2$). ^{19}F NMR (CD_2Cl_2): − 78.9. ^{31}P{^{1}H} NMR (CD_2Cl_2): 120.5. ^{13}C{^{1}H} NMR (CD_2Cl_2): 23.1 (s, CH(CH_3)$_2$), 28.6 (d, 15.5 Hz, C(CH_3)$_3$), 35.4 (d, 30.1 Hz, *C*(CH_3)$_3$), 54.05 (s, *C*(CH_3)$_2$ partly overlapping CD_2Cl_2 signal), 121.3 (q, 320.1 Hz, CF_3SO_3 quartet only partly observable), 121.6 (s, NCHCHN), 127.3 (s, NCHCHN), 140.8 (br, NCHN) X-ray quality crystals could be produced by the cooling of a solution of **1b** in CH_2Cl_2 to −40 °C. Elemental analysis $C_{15}H_{28}N_2F_3O_3PS$ calculated: C 44.55%, H 6.98%, N 6.93% found: C 44.65%, H 7.05%, N 6.87%.

Colorless crystal (polyhedron), dimensions 0.180 × 0.080 × 0.050 mm^3, crystal system orthorhombic, space group $P2_12_12_1$, *Z* = 4, *a* = 16.3820(11) Å, *b* = 10.5135(7) Å, *c* = 11.8675(8) Å, α = 90°, β = 90°, γ = 90°, *V* = 2044.0(2) Å^3, ρ = 1.314 g/cm^3, *T* = 200(2) K, θ_{max} = 25.722°, radiation Mo K$_\alpha$, λ = 0.71073 Å, 0.5° ω-scans with CCD area detector, covering the asymmetric unit in reciprocal space with a mean redundancy of 6.03 and a completeness of 100.0% to a resolution of 0.82 Å, 13 547 reflections measured, 3885 unique (R(int) = 0.0529), 3172 observed ($I > 2\sigma(I)$), μ = 0.28 mm^{-1}, T_{min} = 0.83, T_{max} = 0.96, 226 parameters refined, hydrogen atoms were treated using appropriate riding models, Flack absolute structure parameter −0.01(5), goodness of fit 1.09 for observed reflections, final residual values $R_1(F)$ = 0.065, $wR(F^2)$ = 0.134 for observed reflections, residual electron density −0.56 to 0.59 e·Å^{-3}.

*Synthesis of N-tert-Butyl-N′-di(tert-butyl)phosphino-imidazolium Triflate (**1c**).* To a solution of *N*-*tert*-butylimidazole (8.69 g, 70.0 mmol) and CF_3OSO_2Na (12.65 g, 73.5 mmol) in THF (75 mL) was added at −10 °C di(*tert*-butyl)-chlorophosphine (13.28 g, 73.5 mmol) dissolved in THF (50 mL). The reaction mixture was allowed to warm to room temperature and stirred for 24 h. The solvent was removed *in vacuo*, the solid residue was dissolved in CH_2Cl_2 (100 mL), the insoluble solid was filtered off, washed with CH_2Cl_2 (3 × 10 mL), and the filtrate was concentrated *in vacuo* until crystals started to form and then it was cooled to −40 °C to yield colorless crystals to give **1c** (26.66 g, 91%) ^{1}H NMR (CD_2Cl_2): 8.69 (m, 1H, NC*H*N), 7.85 (m, 1H, $C_{imidazole}$*H*), 7.68 (m, 1H, $C_{imidazole}$*H*), 1.72 (s, 9H, NC(CH_3)$_3$), 1.26 (d, 18H, P(C-(CH_3)$_3$)$_2$. ^{19}F NMR (CD_2Cl_2): − 78.8 ^{31}P{^{1}H} NMR (CD_2Cl_2): 120.2. ^{13}C{^{1}H} NMR (CD_2Cl_2): 28.6 (d, 16.0 Hz,

DOI: 10.1021/acs.inorgchem.5b00513
Inorg. Chem. XXXX, XXX, XXX−XXX

$P(C(CH_3)_3)_2$), 29.9 (s, $N(C(CH_3)_3)$, 35.5 (d, 30.0 Hz, $P(C(CH_3)_3)_2$), 61.6 (s, $N(C(CH_3)_3)$, 121.4 (q, 321.4 Hz, CF_3SO_3 quartet only partly observable), 122.7 (s, NCHCHN), 126.9 (s, NCHCHN), 139.7 (d, 33.6 Hz, NCHN). Elemental analysis $C_{16}H_{30}N_2F_3O_3PS$ calculated: C 45.93%, H 7.23%, N 6.69% Found: C 45.78%, H 7.29%, N 6.92%.

*Synthesis of N-Isopropyl-N′-di(tert-butyl)phosphino-imidazol-2-ylidene (**2b**).* To a suspension of the salt **1b** (6.07 g, 15 mmol) in Et_2O (50 mL) a solution of sodium hexamethyldisilazanide (2.75 g, 15 mmol) in Et_2O (50 mL) was added dropwise at −5 °C over 30 min. The reaction mixture was stirred at 0 °C for 30 min. The solvent was removed *in vacuo* and the residue was extracted with pentane (100 mL). Pentane was removed *in vacuo* and stored at −40 °C. The product could not be crystallized due to its very high solubility, and **2b** was isolated (2.86 g, 11.2 mmol, 75%) as a colorless solid at −40 °C or as a liquid at room temperature and freshly used due to its instability. ^{1}H NMR (THF-d_8): 6.93−7.02 (m, 2H, $C_{imidazole}H$), 4.55 (sept, J = 6.7 Hz, 1H, CH(CH3)2), 1.43 (d, J = 6.7 Hz, 6H, $CH(CH_3)_2$), 1.22 (d, J = 12.3 Hz, 18H, $P(C(CH_3)_3)_2$). ^{31}P{^{1}H}P NMR (THF-d_8): 97.2. ^{13}C{^{1}H} NMR (THF-d_8): 221.6 (br, NCHN), 128.1 (d, J = 34 Hz, NCHCHN), 127.3 (d, 7.9 Hz, NCHCHN), 53.0 (s, $C(CH_3)_2$), 35.3 (d, J = 24.4, $C(CH_3)_3$), 29.6 (d, 16.5 Hz, $C(CH_3)_3$), 24.5 (s, $CH(CH_3)_2$).

*Synthesis of N-tert-Butyl-N′-di(tert-butyl)phosphino-imidazol-2-ylidene (**2c**).* To a suspension of the salt **1c** (4.18 g, 10 mmol) in Et_2O (50 mL) a solution of sodium hexamethyldisilazanide (1.83 g, 10 mmol) in Et_2O (50 mL) was added dropwise at −5 °C over 30 min. The reaction mixture was stirred at 0 °C for 30 min. The solvent was removed *in vacuo*, and the residue extracted with pentane (75 mL). Pentane was removed *in vacuo* to give a viscous oily compound at room temperature which solidified at −40 °C. The product could not be crystallized due to its very high solubility, and **2c** was isolated as a crude colorless solid (2.24 g) at −40 °C. ^{1}H NMR (THF-d_8): 6.93−7.02 (m, 2H, $C_{imidazole}H$), 4.55 (sept, J = 6.7 Hz, 1H, CH(CH3)2), 1.43 (d, J = 6.7 Hz, 6H, $CH(CH_3)_2$), 1.22 (d, J = 12.3 Hz, 18H, $P(C(CH_3)_3)_2$). ^{31}P{^{1}H}P NMR (THF-d_8): 97.2.

*Synthesis of **3a**.* $Ru(PPh_3)_3Cl_2$ (1.44 g, 1.5 mmol) was dissolved in THF (5 mL) to which was added **2a** (357 mg, 1.58 mmol) dissolved in THF (5 mL). The solution was stirred for 1 h. The solution was filtered on a glass sinter and washed with pentane (40 mL) to yield **3a** (848 mg, 1.28 mmol, 86%) as a purple solid. X-ray quality single crystals could be isolated from the layering of CH_2Cl_2 and cyclohexane. ^{1}H NMR (CD_2Cl_2): 7.73 (br, 6H, $P(C_6H_5)_3$), 7.23−7.35 (m, 9H, $P(C_6H_5)_3$), 7.00 (m, 1H, $C_{imidazole}H$), 6.56 (m, 1H, $C_{imidazole}H$), 3.04 (s, 3H, NCH_3), 1.29 (d, J = 13.3 Hz, 9H, $P(C(CH_3)_3)_2$), 1.02 (d, J = 14.9 Hz, 9H, $P(C(CH_3)_3)_2$). ^{31}P{^{1}H} NMR (CD_2Cl_2): 104.2 (d, J = 35.7 Hz, P(C(CH3)3)2), 77.2 (d, J = 35.6 Hz, $P(C(CH_3)_3)_2$). ^{13}C{^{1}H} NMR (CD_2Cl_2): 174.9 (t_{pseudo}, NCN), 133.9 (br, $P(C_6H_5)_3$), 129.5 (m, $P(C_6H_5)_3$), 127.5 (m, $P(C_6H_5)_3$), 125.0 (s, $C_{imidazole}H$), 122.9 (d, J = 8.2 Hz, $C_{imidazole}H$), 44.6 (d, JC,P = 7.3 Hz, $P(C(CH_3)_3)_2$), 36.4 (d, JC,P = 4.5 Hz, $P(C(CH_3)_3)_2$), 34.6 (s, NCH_3), 28.2 (d, J = 5.3 Hz, $P(C(CH_3)_3)_2$), 25.5 (m, $P(C(CH_3)_3)_2$). Note one CH_2Cl_2 in X-ray structure. Elemental analysis $C_{30}H_{38}Cl_2N_2P_2Ru\cdot CH_2Cl_2$ calculated: C 49.95%, H 5.41%, N 3.76%. Elemental analysis $C_{30}H_{38}Cl_2N_2P_2Ru\cdot CH_2Cl_2$ found: C 51.18%, H 5.56%, N 3.67%. EA analysis was consistently problematic with **3a**. Several attempts were made to get better EA data. A representative example is given here.

Violet crystal (polyhedron), dimensions 0.08 × 0.07 × 0.05 mm^3, crystal system monoclinic, space group $P2_1/n$, Z = 4, a = 9.9759(7) Å, b = 16.3832(12) Å, c = 23.1814(17) Å, α = 90°, b = 95.333(2)°, γ = 90°, V = 3772.3(5) Å^3, ρ = 1.462 g/cm^3, T = 200(2) K, θ_{max} = 23.81°, radiation Mo K$_\alpha$, λ = 0.71073 Å, 0.5° ω-scans with CCD area detector, covering the asymmetric unit in reciprocal space with a mean redundancy of 5.41 and a completeness of 100.0% to a resolution of 0.88 Å, 33690 reflections measured, 5796 unique (R(int) = 0.0940), 4147 observed ($I > 2\sigma$(I)), μ = 0.95 mm^{-1}, T_{min} = 0.93, T_{max} = 0.95, 417 parameters refined, hydrogen atoms were treated using appropriate riding models, goodness of fit 1.08 for observed reflections, final residual values $R_1(F)$ = 0.061, $wR(F^2)$ = 0.132 for observed reflections, residual electron density −1.11 to 0.83 e·Å^{-3}.

*Synthesis of **3b**.* $Ru(PPh3)_3Cl_2$ (9.35 g, 9.75 mmol) was dissolved in THF (50 mL) to which was added **2b** (2.68 g, 10.5 mmol) dissolved in THF (25 mL). The solution was stirred for 1 h. Half of the solution was removed *in vacuo*, filtered on a glass sinter, and washed with pentane (40 mL) to yield **3b** (5.34 g, 7.75 mmol, 79%) as a purple solid. X-ray quality single crystals could be isolated from the layering of CH_2Cl_2 and cyclohexane. ^{1}H NMR (CD_2Cl_2): 7.65 (br, 6H, $P(C_6H_5)_3$), 7.22−7.33 (m, 9H, $P(C_6H_5)_3$), 7.07 (s, 1H, $C_{imidazole}H$), 6.80 (s, 1H, $C_{imidazole}H$), 4.94 (sept, J = 6.8 Hz, 1H, $CH(CH_3)_2$), 1.26−1.31 (m, 12H, $P(C(CH_3)_3)_2$ and $CH(CH_3)_2$), 1.05 (d, J = 14.7 Hz, 9H, $P(C(CH_3)_3)_2$), 0.77 (d, J = 6.7 Hz, 3H, $CH(CH_3)_2$). ^{31}P{^{1}H} NMR (CD_2Cl_2): 108.8 (d, J = 37.3 Hz, $P(C(CH_3)_3)_2$), 77.7 (d, J = 37.3 Hz, $P(C_6H_5)_3$). ^{13}C{^{1}H} NMR (CD_2Cl_2): 173.9 (m, NCN), 134.1 (d, J = 9.2 Hz, $P(C_6H_5)_3$), 129.5 (d, J = 2.5 Hz, $P(C_6H_5)_3$), 127.5 (d, J = 10.4 Hz, $P(C_6H_5)_3$), 123.6 (d, J = 8.0 Hz, $C_{imidazole}$H), 119.5 (br, $C_{imidazole}$H), 49.8 (s, $CH(CH_3)_2$), 44.6 (d, J = 7.7 Hz, $P(C(CH_3)_3)_2$), 36.9 (d, J = 3.5 Hz, $P(C(CH_3)_3)_2$), 28.4 (d, J = 5.3 Hz, $P(C(CH_3)_3)_2$), 26.2 (m, $P(C(CH_3)_3)_2$), 25.1 (s, $CH(CH_3)_2$), 20.4 (s, $CH(CH_3)_2$). Note one CH_2Cl_2 and THF in NMR spectra. Elemental Analysis $C_{32}H_{42}Cl_2N_2P_2Ru\cdot CH_2Cl_2\cdot$THF calculated: C, 52.55%; H, 6.20%; N, 3.31% Elemental analysis $C_{32}H_{42}Cl_2N_2P_2Ru\cdot CH_2Cl_2\cdot$THF found: C 52.63%, H 6.39%, N 3.39%.

Violet crystal (plate), dimensions 0.120 × 0.080 × 0.070 mm^3, crystal system triclinic, space group $P\bar{1}$, Z = 4, a = 11.6983(5) Å, b = 17.3524(8) Å, c = 17.5483(8) Å, α = 85.5090(12)°, β = 82.1460(12)°, γ = 78.1590(12)°, V = 3449.0(3) Å^3, ρ = 1.394 g/cm^3, T = 200(2) K, θ_{max} = 25.055°, radiation Mo K$_\alpha$, λ = 0.71073 Å, 0.5° ω-scans with CCD area detector, covering the asymmetric unit in reciprocal space with a mean redundancy of 2.71 and a completeness of 99.8% to a resolution of 0.84 Å, 33075 reflections measured, 12 204 unique (R(int) = 0.0651), 7929 observed ($I > 2\sigma(I)$), μ = 0.73 mm^{-1}, T_{min} = 0.86, T_{max} = 0.96, 832 parameters refined, hydrogen atoms were treated using appropriate riding models, goodness of fit 0.98 for observed reflections, final residual values $R_1(F)$ = 0.045, $wR(F^2)$ = 0.079 for observed reflections, residual electron density −0.47 to 0.50 e·Å^{-3}.

*Synthesis of **3c**.* $Ru(PPh_3)_3Cl_2$ (9.96 g, 10.39 mmol) was dissolved in THF (50 mL) to which was added **2c** (3.01 g, 11.2 mmol) dissolved in THF (5 mL). The solution was stirred for 1 h. The majority of the solution was removed *in vacuo*, filtered on a glass sinter, and washed with pentane (50 mL) to yield **3c** (4.05 g, 5.8 mmol, 56%) as a purple solid. X-ray quality single crystals were isolated from the layering of CH_2Cl_2 and

DOI: 10.1021/acs.inorgchem.5b00513
Inorg. Chem. XXXX, XXX, XXX−XXX

cyclohexane. ^{1}H NMR (CD_2Cl_2): 7.50−8.10 (br, 4H, P-(C_6H_5)$_3$), 7.03−7.49 (m, 12H, P(C_6H_5)$_3$ and $C_{imidazole}H$), 6.45−6.85 (br, 1H, P(C_6H_5)$_3$), 1.33−1.45 (m, 18H, N−C(CH_3)$_3$ and P(C(CH_3)$_3$)$_2$), 1.05 (d, J = 14.9 hz, 9H, P(C(CH_3)$_3$)$_2$). ^{31}P{^{1}H} NMR (CD_2Cl_2): 110.8 (d, J = 41.5 Hz, P(C(CH_3)$_3$)$_2$), 72.6 (d, J = 41.4 Hz, P(C_6H_5)$_3$). ^{13}C{^{1}H} NMR (CD_2Cl_2): 171.4 (m, NCN), 135.2 (m, P(C_6H_5)$_3$), 130.1 (m, P(C_6H_5)$_3$), 128.0 (m, P(C_6H_5)$_3$), 122.7 (d, J = 7.0 Hz, $C_{imidazole}$H), 121.9 (d, J = 1.5 Hz, $C_{imidazole}$H), 59.7 (s, N-C(CH_3)$_3$), 43.8 (d, J = 10.5 Hz, P-C(CH_3)$_3$), 37.3 (s, N−C(CH_3)$_3$), 30.1 (s, N−C(CH_3)$_3$), 29.1 8 (d, J = 5.0 Hz, P−C(CH_3)$_3$), 27.0 (d, J = 3.6 Hz, P−C(CH_3)$_3$). Elemental analysis $C_{33}H_{44}Cl_2N_2P_2Ru$ calculated: C 56.41%, H 6.31%, N 3.99% Found: C 56.65%, H 6.61%, N 4.17%.

Violet crystal (plate), dimensions 0.090 × 0.080 × 0.060 mm^3, crystal system monoclinic, space group $P2_1$, Z = 4, a = 10.5570(10) Å, b = 17.4081(17) Å, c = 19.9446(18) Å, α = 90°, β = 91.141(2)°, γ = 90°, V = 3664.6(6) Å^3, ρ = 1.427 g/cm^3, T = 200(2) K, θ_{max} = 24.807°, radiation Mo K$_\alpha$, λ = 0.71073 Å, 0.5° ω-scans with CCD area detector, covering the asymmetric unit in reciprocal space with a mean redundancy of 3.33 and a completeness of 99.5% to a resolution of 0.85 Å, 21833 reflections measured, 12376 unique (R(int) = 0.0712), 8056 observed ($I > 2\sigma(I)$), μ = 0.83 mm^{-1}, T_{min} = 0.75, T_{max} = 0.96, 775 parameters refined, hydrogen atoms were treated using appropriate riding models, Flack absolute structure parameter 0.13(3), goodness of fit 1.03 for observed reflections, final residual values $R_1(F)$ = 0.076, $wR(F^2)$ = 0.106 for observed reflections, residual electron density −1.13 to 1.14 e·Å^{-3}.

Synthesis of ***4a$_H$***. **3a** (280 mg, 0.42 mmol) was dissolved in pyridine (3 mL) without stirring. Within 30 min orange crystals formed. The pyridine was decanted and hexanes (15 mL) was added, stirred, and filtered to isolate **4a$_H$** (203 mg, 0.365 mmol, 87%) as orange crystals. X-ray quality single crystals were isolated from the layering of CH_2Cl_2 and cyclohexane. ^{1}H NMR (C_5D_5N): 8.73 (m, $C_5D_5N_{residual}$ and C_5H_5N), 8.23 (m, $CH_{imidazole}$), 7.99 (s, $CH_{imidazole}$), 7.98 (s, $CH_{imidazole}$), 7.90 (s, $CH_{imidazole}$), 7.59 (m, $C_5D_5N_{residual}$ and C_5H_5N), 7.22 (m, $C_5D_5N_{residual}$ and C_5H_5N), 4.68 (s, CH_3), 4.26 (s, CH_3), 1.03 (m, P(C(CH_3)$_3$)$_2$). ^{31}P{^{1}H} NMR (C_5D_5N): 113.9, 107.5. ^{13}C{^{1}H} NMR (C_5D_5N): 179.0 (d, J = 13.9 Hz, NCN), 177.7 (d, J = 13.3 Hz, NCN), 150.1, 150.0, 135.8, 135.6, 128.1 (s, $CH_{imidazole}$), 128.0 (s, $CH_{imidazole}$), 125.7 (d, J = 7.2 Hz, $CH_{imidazole}$), 125.2 (d, J = 7.2 Hz, $CH_{imidazole}$), 123.9, 123.6, 41.3 (d, J = 2.2 Hz, P(C(CH_3)$_3$)$_2$), 40.0 (d, J = 2.1 Hz, P(C(CH_3)$_3$)$_2$), 36.9 (s, CH_3), 35.7 (s, CH_3), 29.3 (d, J = 5.2 Hz, P(C(CH_3)$_3$)$_2$), 29.0 (d, J = 5.2 Hz, P(C(CH_3)$_3$)$_2$). Elemental analysis $C_{22}H_{33}Cl_2N_4PRu{\cdot}2CH_2Cl_2$ calculated: C 39.69%, H 5.31%, N 7.71% Found: C 40.36%, H 5.21%, N 7.99%. As in the elemental analysis of **3a** repeated attempts were made to obtain better EA data but results were inconsistent, presumably due to residual solvent.

Orange crystal (polyhedron), dimensions 0.26 × 0.16 × 0.16 mm^3, crystal system monoclinic, space group $P2_1/c$, Z = 4, a = 8.6967(7) Å, b = 15.7760(12) Å, c = 22.6971(17) Å, α = 90°, β = 93.707(1)°, γ = 90°, V = 3107.5(4) Å^3, ρ = 1.552 g/cm^3, T = 199(2) K, θ_{max} = 28.71°, radiation Mo K$_\alpha$, λ = 0.71073 Å, 0.5° ω-scans with CCD area detector, covering the asymmetric unit in reciprocal space with a mean redundancy of 4.68 and a completeness of 99.1% to a resolution of 0.74 Å, 38123 reflections measured, 7973 unique (R(int) = 0.0573), 6072 observed ($I > 2\sigma(I)$), μ = 1.09 mm^{-1}, T_{min} = 0.76, T_{max} = 0.84, 332 parameters refined, hydrogen atoms were treated using appropriate riding models, goodness of fit 1.03 for observed reflections, final residual values $R_1(F)$ = 0.038, $wR(F^2)$ = 0.073 for observed reflections, residual electron density −0.99 to 1.22 e·Å^{-3}.

Synthesis of ***4a$_{Br}$***. **3a** (2.15 g, 3.25 mmol) was dissolved in 3-bromopyridine (2−3 mL) without stirring. Within 30 min orange crystals formed. The 3-bromopyridine was decanted and Et$_2$O (2 × 15 mL) was added, stirred, and filtered to isolate **4a$_{Br}$** (1.89 g, 2.64 mmol, 82%) as orange crystals.The crystals initially formed were of sufficient quality for single crystal X-ray diffraction. ^{1}H NMR (C_5D_5N): 11.2, 8.83 (m, free 3-bromopyridine), 8.74 (residual pyridine), 8.60 (m, free 3-bromopyridine), 8.09, 7.91, 7.85−7.81 (m, free 3-bromopyridine), 7.73, 7.59 (residual pyridine), 7.22 (residual pyridine), 7.18−7.12 (m, free 3-bromopyridine), 6.98, 6.60, 4.67, 4.25, 3.78, 3.61, 1.43 (d, 12.2 Hz, P(C(CH3)3)), 1.37 (d, 11.9 Hz, P(C(CH3)3)), 1.06 (d, 13.5 Hz, P(C(CH3)3)), 1.05 (d, 13.7 Hz, P(C(CH3)3)). ^{31}P{^{1}H} NMR (C_5D_5N): 115.8, 109.3, 89.0, 64.6. ^{13}C{^{1}H} NMR (C_5D_5N): 184.1, 180.6, 179.4, 152.5, 149.7, 140.1, 130.0, 129.4, 129.2, 128.5, 127.1, 126.7, 122.5, 119.1, 42.8, 42.5, 42.4, 41.6, 39.3, 38.3, 37.2, 30.85, 30.81, 30.77, 30.51, 30.46. Elemental analysis $C_{22}H_{31}Br_2Cl_2N_4PRu$ calculated: C 36.99%, H 4.37%, N 7.84% Found: C 37.04%, H 4.32%, N 8.04%.

Orange crystal (polyhedron), dimensions 0.17 × 0.12 × 0.11 mm^3, crystal system monoclinic, space group Cc, Z = 4, a = 18.609(3) Å, b = 19.892(3) Å, c = 8.7676(15) Å, α = 90°, β = 113.047(3)°, γ = 90°, V = 2986.5(9) Å^3, ρ = 1.589 g/cm^3, T = 200(2) K, θ_{max} = 25.95°, radiation Mo K$_\alpha$, λ = 0.71073 Å, 0.5° ω-scans with CCD area detector, covering the asymmetric unit in reciprocal space with a mean redundancy of 2.90 and a completeness of 97.7% to a resolution of 0.82 Å, 8498 reflections measured, 2864 unique (R(int) = 0.0640), 2499 observed ($I > 2\sigma(I)$), μ = 3.45 mm^{-1}, T_{min} = 0.59, T_{max} = 0.70, 310 parameters refined, hydrogen atoms were treated using appropriate riding models, Flack absolute structure parameter 0.46(3), goodness of fit 1.06 for observed reflections, final residual values $R_1(F)$ = 0.045, $wR(F^2)$ = 0.086 for observed reflections, residual electron density −0.81 to 0.72 e·Å^{-3}.

Synthesis of ***4b$_{Br}$***. **3b** (1.26 g, 1.83 mmol) was dissolved in 3-bromopyridine (3 mL) without stirring. Within 30 min orange crystals formed. The 3-bromopyridine was decanted and Et2O (3 × 20 mL) was added, stirred, and filtered to isolate **4b$_{Br}$** (1.28 g, 1.72 mmol, 94%) as orange crystals. ^{1}H NMR (CD_2Cl_2): 10.45, 10.37, 10.30, 9.24, 9.18, 8.97, 8.91, 8.67, 8.51, 8.20, 8.10, 7.83, 7.68, 7.27, 7.21, 7.09, 6.92, 6.87, 5.96 (m, NCH(CH_3)$_2$), 4.23 (m, NCH(CH_3)$_2$), 1.56−1.33 (m, NCH-(CH_3)$_2$) and P(C(CH_3)$_3$)$_2$), 1.03 (m, NCH(CH_3)$_2$) and P(C(CH_3)$_3$)$_2$). ^{31}P{^{1}H} NMR (CD_2Cl_2): 122.1, 120.0, 119.9. ^{13}C{^{1}H} NMR (CD_2Cl_2): 184.3 (m, NCN), 158.4, 157.9, 157.4, 156.4, 154.5, 153.7, 151.0, 148.0, 138.5, 138.2, 137.9, 124.9, 124.7, 124.6, 124.1, 120.8, 119.2, 118.8, 118.1, 50.6, 49.4, 41.0, 40.3, 30.0 (d, 5.7 Hz), 29.7, 23.6, 23.5. Elemental analysis $C_{24}H_{35}Br_2Cl_2N_4PRu$ calculated: C 38.83%, H 4.75%, N 7.55% Found: C 38.79%, H 4.71%, N 7.64%.

Synthesis of ***4c$_{Br}$***. **3c** (1.44 g, 2.05 mmol) was dissolved in 3-bromopyridine (3 mL) without stirring. Within 30 min orange crystals formed. The 3-bromopyridine was decanted and Et$_2$O (10 mL) was added, stirred, and filtered to isolate **4c$_{Br}$** (1.43 g, 1.89 mmol, 92%) as orange crystals. The crystals initially formed were of sufficient quality for single crystal X-ray diffraction. ^{1}H NMR (NC_5D_5): 8.84 (d, J = 2.5 Hz, free 3-bromopyridine), 8.74 (s, residual pyridine), 8.60 (dd, J = 4.7

DOI: 10.1021/acs.inorgchem.5b00513
Inorg. Chem. XXXX, XXX, XXX−XXX

and 1.3 Hz, free 3-bromopyridine), 7.84−7.77 (m, free 3-bromopyridine), 7.59 (s, residual pyridine), 7.55 (d, J = 2.1 Hz, $CH_{imidazole}$), 7.53 (m, $CH_{imidazole}$), 7.49 (d, J = 2.2 Hz, $CH_{imidazole}$), 7.46 (d, J = 2.3 Hz, $CH_{imidazole}$), 7.24 (d, J = 2.2 Hz, $CH_{imidazole}$), 7.22 (s, residual pyridine), 7.14 (3-bromopyridine), 1.94, 1.82, 1.77, 1.58, 1.55, 1.52, 1.50, 1.48, 1.46, 1.40, 1.36, 1.30, 1.26, 1.19, 1.15, 1.12, 1.09 $^{31}P\{^1H\}$ NMR (CD_2Cl_2): 132.45, 132.37, 132.1, 122.82. $^{13}C\{^1H\}$ NMR (CD_2Cl_2): 181.5, 175.6, 152.5, 149.7, 140.1, 126.7, 124.2, 123.9, 122.5, 122.4, 60.1, 59.8, 59.77, 58.4, 42.9, 42.8, 42.6, 42.5, 42.4, 42.2, 42.1, 42.0, 41.95, 32.4, 32.2, 32.0 (d, J = 5.3 Hz), 31.8 (d, J = 5.4 Hz), 30.4 (d, J = 4.9 Hz), 30.3 (d, J = 4.4 Hz), 30.1 (d, J = 4.9 Hz), 30.0 (d, J = 4.6 Hz), 28.9. Elemental Analysis $C_{25}H_{37}Br_2Cl_2N_4PRu$ calculated: C 39.70%, H 4.93%, N 7.41% Found: C 40.15%, H 4.59%, N 7.65%.

Orange crystal (needle), dimensions 0.940 × 0.130 × 0.060 mm^3, crystal system triclinic, space group $P\bar{1}$, Z = 2, a = 8.987(2) Å, b = 13.992(3) Å, c = 14.689(3) Å, α = 82.541(4)°, β = 86.686(4)°, γ = 75.254(4)°, V = 1770.6(7) Å^3, ρ = 1.715 g/cm^3, T = 199(2) K, θ_{max} = 27.743°, radiation Mo K$_\alpha$, λ = 0.71073 Å, 0.5° ω-scans with CCD area detector, covering the asymmetric unit in reciprocal space with a mean redundancy of 2.83 and a completeness of 97.6% to a resolution of 0.73 Å, 23079 reflections measured, 8142 unique (R(int) = 0.0523), 5730 observed ($I > 2\sigma(I)$), μ = 4.05 mm^{-1}, T_{min} = 0.52, T_{max} = 0.77, 388 parameters refined, hydrogen atoms were treated using appropriate riding models, goodness of fit 1.06 for observed reflections, final residual values $R_1(F)$ = 0.051, $wR(F^2)$ = 0.099 for observed reflections, residual electron density −0.97 to 1.02 e·Å^{-3}.

Synthesis of ***5a***. $\mathbf{4a_{Br}}$ (950 mg, 1.33 mmol) was dissolved in CH_2Cl_2 (20 mL) and cooled to −40 °C. Trimethylsilyldiazomethane (0.70 mL, 2 M hexanes solution) was added, and the solution was allowed to warm to room temperature. Once noticeable bubbling had ceased the solution was stirred for an additional hour. The solvent was removed *in vacuo*. The solid was slurried in a minimum amount of THF and filtered. **5a** was washed off of the filter with CH_2Cl_2 (10 mL) and the solvent removed *in vacuo*. The sample was further purified via crystallization from CH_2Cl_2 and cyclohexane to yield **5a** (310 mg, 0.64 mmol, 47%) as green crystals. . X-ray quality single crystals were isolated from the layering of CH_2Cl_2 and cyclohexane. ^1H NMR (CD_2Cl_2): 18.61 (d, J = 6.2 Hz, ^1H, RuC*H*), 7.23 (m, ^1H, $C_{imidazole}H$), 6.91 (d, ^1H, $C_{imidazole}H$), 3.52 (s, 3H, NCH_3), 1.55 (d, J = 15.1, 9H, $P(C(CH_3)_3)_2$), 1.22 (d, J = 15.9 Hz, 9H, $P(C(CH_3)_2)$, 0.37 (s, $Si(CH_3)_3$). $^{31}P\{^1H\}$ NMR (CD_2Cl_2): 142.2 $^{13}C\{^1H\}$ NMR (CD_2Cl_2): 168.5 (d, J = 20.6 Hz, N*C*N), 125.4 (d, J = 2.4 Hz, NC*C*N), 123.3 (d, J = 7.8 Hz, NC*C*N), 40.8 (d, JC,P = 9.5 Hz, $P(C(CH_3)_3)_2$), 38.6 (d, JC,P = 5.1 Hz, $P(C(CH_3)_3)_2$), 35.7 (s, NCH_3), 28.5 (d, J = 4.0 Hz, $P(C(CH_3)_3)_2$), 28.2 (d, J = 5.0 Hz, $P(C(CH_3)_3)_2$). Elemental analysis $C_{16}H_{33}Cl_2N_2PRuSi$ calculated: C 39.67%, H 6.87%, N 5.78% Found: C 40.24%, H 6.88%, N 5.69%.

Green crystal (polyhedron), dimensions 0.110 × 0.100 × 0.100 mm^3, crystal system monoclinic, space group $P2_1/n$, Z = 4, a = 9.8131(13) Å, b = 15.449(2) Å, c = 19.426(3) Å, α = 90°, β = 93.744(3)°, γ = 90°, V = 2938.8(7) Å^3, ρ = 1.479 g/cm^3, T = 200(2) K, θ_{max} = 25.680°, radiation Mo K$_\alpha$, λ = 0.71073 Å, 0.5° ω-scans with CCD area detector, covering the asymmetric unit in reciprocal space with a mean redundancy of 3.25 and a completeness of 100.0% to a resolution of 0.82 Å, 18438 reflections measured, 5574 unique (R(int) = 0.0889), 3664 observed ($I > 2\sigma(I)$), μ = 1.18 mm^{-1}, T_{min} = 0.76, T_{max} = 0.91, 328 parameters refined, hydrogen atoms were treated using appropriate riding models, goodness of fit 1.04 for observed reflections, final residual values $R_1(F)$ = 0.056, $wR(F^2)$ = 0.109 for observed reflections, residual electron density −0.69 to 0.61 e·Å^{-3}.

Synthesis of ***5b***. $\mathbf{4b_{Br}}$ (350 mg, 0.47 mmol) was dissolved in CH_2Cl_2 (20 mL) and cooled to −40 °C. Trimethylsilyldiazomethane (0.25 mL, 2 M hexanes solution)was added, and the solution was allowed to warm to room temperature. Once noticeable bubbling had ceased the solution was stirred for an additional hour. The solvent was removed *in vacuo*. The solid was slurried in a minimum amount of THF and filtered. **5b** was washed off the filter with CH_2Cl_2 (10 mL), and the solvent was removed *in vacuo*. The sample was further purified via crystallization from CH_2Cl_2 and cyclohexane to yield **5b** (145 mg, 0.28 mmol, 60%) as green crystals. X-ray quality single crystals were isolated from the layering of CH_2Cl_2 and cyclohexane. ^1H NMR (CD_2Cl_2): 18.56 (d, J = 6.3 Hz, 1H, RuCH), 7.28 (m, 1H, $C_{imidazole}H$), 7.03 (d, J = 2.1 Hz, 1H, $C_{imidazole}H$), 4.61 (sept, J = 6.8 Hz, 1H, $CH(CH_3)_2$), 1.55 (d, J = 15.3 Hz, 9H, $P(C(CH_3)_3)_2$), 1.23 (d, J = 16.1 Hz, 9H, $P(C(CH_3)_3)_2$), 0.37 (s, 9H, $Si(CH_3)_3$) $^{31}P\{^1H\}$ NMR (CD_2Cl_2): 141.8. $^{13}C\{^1H\}$ NMR (CD_2Cl_2): 215.9 (br), 165.5 (d, J = 20.6 Hz, NCN), 122.1 (d, J = 7.4 Hz, NCCN), 118.5 (d, J = 2.5 Hz, NCCN), 49.0 (s,), 39.4 (d, J = 9.9 Hz), 37.1 (d, J = 4.6 Hz), 26.9 (dd, J = 15.4/4.3 Hz), 21.5 (d, J = 22.4 Hz), −3.3 (s). Elemental analysis $C_{18}H_{37}Cl_2N_2PRuSi$ calculated: C 42.18%, H 7.28%, N 5.47% Found: C 42.43%, H 7.26%, N 5.42%.

Green crystal (polyhedron), dimensions 0.130 × 0.090 × 0.060 mm^3, crystal system triclinic, space group $P\bar{1}$, Z = 2, a = 9.0506(3) Å, b = 9.7152(3) Å, c = 15.2604(4) Å, α = 94.5103(15)°, β = 94.3406(15)°, γ = 113.3483(13)°, V = 1219.73(6) Å^3, ρ = 1.395 g/cm^3, T = 200(2) K, θ_{max} = 32.245°, radiation Mo Kα, λ = 0.71073 Å, 0.5° ω-scans with CCD area detector, covering the asymmetric unit in reciprocal space with a mean redundancy of 2.86 and a completeness of 100.0% to a resolution of 0.67 Å, 24766 reflections measured, 8543 unique (R(int) = 0.0299), 7381 observed ($I > 2\sigma(I)$), μ = 0.98 mm^{-1}, T_{min} = 0.87, T_{max} = 0.96, 237 parameters refined, hydrogen atoms were treated using appropriate riding models, goodness of fit 1.04 for observed reflections, final residual values $R_1(F)$ = 0.031, $wR(F^2)$ = 0.065 for observed reflections, residual electron density −0.34 to 0.67 e·Å^{-3}.

Synthesis of ***5c***. $\mathbf{4c_{Br}}$ (420 mg, 0.56 mmol) was dissolved in CH_2Cl_2 (15 mL) and cooled to −40 °C. Trimethylsilyldiazomethane (0.21 mL, 2 M hexanes solution) was added, and the solution was allowed to warm to room temperature. Once noticeable bubbling had ceased the solution was stirred for an additional hour. The solvent was removed *in vacuo*. The solid was slurried in a minimum amount of THF and filtered. **5c** was washed off the filter with CH_2Cl_2 (10 mL), and the solvent was removed *in vacuo*. The sample was further purified via crystallization from CH_2Cl_2 and cyclohexane to yield **5c** (266 mg, 0.51 mmol, 91%) as green crystals. . ^1H NMR (CD_2Cl_2): 18.98 (d, J = 5.7 Hz, 1H, RuCH), 7.23 (m, 1H, $C_{imidazole}H$), 7.15 (d, J = 2.2 Hz, 1H, $C_{imidazole}H$), 1.60 (d, J = 15.3 Hz, 9H, $P(C(CH_3)_3)_2$), 1.43 (s, 9H, $NC(CH_3)_3$), 1.23 (d, J = 16.1 Hz, 9H, $P(C(CH_3)_3)_2$), 0.38 (s, 9H, $Si(CH_3)_3$). $^{31}P\{^1H\}$ NMR (CD_2Cl_2): 136.5. $^{13}C\{^1H\}$ NMR (CD_2Cl_2): 164.9 (m, NCN), 121.1 (m, $C_{imidazole}H$), 59.0 (s, N-$C(CH_3)_3$), 40.0 (d, J = 11.8 Hz, P-$C(CH_3)_3$), 38.2 (d, J = 7.8 Hz, P-$C(CH_3)_3$), 29.7 (s, N−$C(CH_3)_3$), 28.1 (d, J = 4.1 Hz, P−$C(CH_3)_3$), 27.7 (d, J = 4.7

DOI: 10.1021/acs.inorgchem.5b00513
Inorg. Chem. XXXX, XXX, XXX−XXX

Hz, P−C(CH_3)$_3$), −2.1 (s, Si(CH_3)$_3$). The alkylidene C was not observed. Elemental analysis $C_{19}H_{39}Cl_2N_2PRuSi$ calculated: C 43.34%, H 7.47%, N 5.32% Found: C 43.34%, H 7.49%, N 5.56%.

Synthesis of **6c**. $\mathbf{4c_{Br}}$ (2.05 g, 2.71 mmol) was dissolved in CH_2Cl_2 (50 mL) and cooled to −40 °C. Phenyldiazomethane (0.4 g, 3.39 mmol, 1.25 equiv) was added, and the solution was allowed to warm to room temperature. Once noticeable bubbling had ceased the solution was stirred for an additional hour. The solvent was removed *in vacuo*. The solid was slurried in a minimum amount of THF and filtered. The sample was further purified via crystallization from CH_2Cl_2 and cyclohexane to yield **5c** (1.12 g, 2.11 mmol, 78%) as green crystals. . ^{1}H NMR (CD_2Cl_2): 15.77 (d, J = 10.2 Hz, 1H, RuC*H*), 8.39 (d, J = 10.2 Hz, 1H, RuC*H*), (d, J = 7.8 Hz, 2H, *o*-Ph), 7.70 (t, J = 7.5 Hz, 1H, *p*-Ph), 7.45 (t, J = 7.8 Hz, 2H, m-Ph), (m, J = 2.1 Hz, 1H, C$H_{Imidazole}$), 7.19 (d, J = 7.5 Hz, 1H, C$H_{Imidazole}$), 1.62 (d, J = 14.7 Hz, 9H, P−C(CH_3)$_3$), 1.42(s, 9H, N−C(CH_3)$_3$), 1.30(d, J = 15.8 Hz, 9H, P−C(CH_3)$_3$). ^{31}P{^{1}H} NMR (CD_2Cl_2): 129.8. ^{13}C{^{1}H} NMR (CD_2Cl_2): 299.1 (d, J = 14.0 Hz, CHPh), 167.3 (d, J = 16.5 Hz, NCHN), 150.9 (d, J = 14.0 Hz, CH-*ipso*-C_6H_5), 131.6 (s, Ph), 130.5 (s, Ph), 129.1 (s, Ph), 121.9 (d, J = 7.0 Hz, $CH_{Imidazole}$), 121.5 (d, J = 2.4 Hz, $CH_{Imidazole}$), 59.4 (s, N-*C*(CH_3)$_3$), 41.1 (d, J = 10.8 Hz, P-*C*(CH_3)$_3$), 39.5 (d, J = 5.3 Hz, P-*C*(CH_3)$_3$), 30.0 (s, N−C(CH_3)$_3$), 28.8 (d, J = 4.5 Hz, P−C(CH_3)$_3$), 28.2 (d, J = 4.0 Hz, P−C(CH_3)$_3$). Elemental analysis $C_{19}H_{39}Cl_2N_2PRuSi$ calculated: C 49.81%, H 6.65%, N 5.28% Found: C 49.82%, H 6.89%, N 5.06%.

■ ASSOCIATED CONTENT

Ⓢ Supporting Information

The Supporting Information is available free of charge on the ACS Publications website at DOI: 10.1021/acs.inorgchem.5b00513.

Experimental NMR data for compounds **1** and **3**−**5**. Tables of crystallographic data. Further details of GC analysis (PDF)
(CIF)

■ AUTHOR INFORMATION

Corresponding Author

*E-mail: chrisc.brown@alum.utoronto.ca.

Notes

The authors declare no competing financial interest.

■ ACKNOWLEDGMENTS

C.C.B., M.L. and P.H. worked at CaRLa (Catalysis Research Laboratory) of Heidelberg University, being cofinanced by the University of Heidelberg, the State of Baden-Wuerttemberg, and BASF SE. We gratefully acknowledge generous support from these institutions.

■ DEDICATION

$^{\perp}$We dedicate this paper to the memory of Prof. Dr. Peter Hofmann.

■ REFERENCES

(1) Schwab, P.; France, M. B.; Ziller, J. W.; Grubbs, R. H. *Angew. Chem., Int. Ed. Engl.* **1995**, *34* (18), 2039−2041.

(2) (a) Scholl, M.; Ding, S.; Lee, C. W.; Grubbs, R. H. *Org. Lett.* **1999**, *1* (6), 953−956. (b) Ackermann, L.; Fürstner, A.; Weskamp, T.; Kohl, F. J.; Herrmann, W. A. *Tetrahedron Lett.* **1999**, *40* (26), 4787−4790.

(3) (a) Love, J. A.; Morgan, J. P.; Trnka, T. M.; Grubbs, R. H. *Angew. Chem., Int. Ed.* **2002**, *41* (21), 4035−4037. (b) Trnka, T. M.; Dias, E. L.; Day, M. W.; Grubbs, R. H. *ARKIVOC* **2003**, *2002*, 28−41.

(4) (a) Conrad, J. C.; Amoroso, D.; Czechura, P.; Yap, G. P. A.; Fogg, D. E. *Organometallics* **2003**, *22* (18), 3634−3636. (b) Dias, E. L.; Nguyen, S. T.; Grubbs, R. H. *J. Am. Chem. Soc.* **1997**, *119* (17), 3887−3897.

(5) (a) Katayama, H.; Nagao, M.; Ozawa, F. *Organometallics* **2003**, *22* (3), 586−593. (b) Kingsbury, J. S.; Harrity, J. P. A.; Bonitatebus, P. J.; Hoveyda, A. H. *J. Am. Chem. Soc.* **1999**, *121* (4), 791−799. (c) Schwab, P.; Grubbs, R. H.; Ziller, J. W. *J. Am. Chem. Soc.* **1996**, *118* (1), 100−110.

(6) Van Veldhuizen, J. J.; Campbell, J. E.; Giudici, R. E.; Hoveyda, A. H. *J. Am. Chem. Soc.* **2005**, *127* (18), 6877−6882.

(7) Herrmann, W. A.; Köcher, C.; Gooßen, L. J.; Artus, G. R. J. *Chem. - Eur. J.* **1996**, *2* (12), 1627−1636.

(8) (a) Cabeza, J. A.; Damonte, M.; García-Álvarez, P.; Kennedy, A. R.; Pérez-Carreño, E. *Organometallics* **2011**, *30* (4), 826−833. (b) Focken, T.; Raabe, G.; Bolm, C. *Tetrahedron: Asymmetry* **2004**, *15* (11), 1693−1706. (c) Ho, C.-C.; Chatterjee, S.; Wu, T.-L.; Chan, K.-T.; Chang, Y.-W.; Hsiao, T.-H.; Lee, H. M. *Organometallics* **2009**, *28* (9), 2837−2847. (d) Naziruddin, A. R.; Hepp, A.; Pape, T.; Hahn, F. E. *Organometallics* **2011**, *30* (21), 5859−5866. (e) Wheaton, C. A.; Bow, J.-P. J.; Stradiotto, M. *Organometallics* **2013**, *32* (21), 6148−6161. (f) Yang, C.; Lee, H. M.; Nolan, S. P. *Org. Lett.* **2001**, *3* (10), 1511−1514.

(9) (a) Benhamou, L.; Wolf, J.; César, V.; Labande, A. s.; Poli, R.; Lugan, N. l.; Lavigne, G. *Organometallics* **2009**, *28* (24), 6981−6993. (b) Hahn, F. E.; Naziruddin, A. R.; Hepp, A.; Pape, T. *Organometallics* **2010**, *29* (21), 5283−5288. (c) Cabeza, J. A.; Damonte, M.; García-Álvarez, P.; Hernández-Cruz, M. G.; Kennedy, A. R. *Organometallics* **2012**, *31* (1), 327−334.

(10) Salem, H.; Schmitt, M.; Herrlich, U.; Kühnel, E.; Brill, M.; Nägele, P.; Bogado, A. L.; Rominger, F.; Hofmann, P. *Organometallics* **2013**, *32* (1), 29−46.

(11) (a) Hansen, S. M.; Rominger, F.; Metz, M.; Hofmann, P. *Chem. - Eur. J.* **1999**, *5* (2), 557−566. (b) Hansen, S. M.; Volland, M. A. O.; Rominger, F.; Eisenträger, F.; Hofmann, P. *Angew. Chem., Int. Ed.* **1999**, *38* (9), 1273−1276. (c) Volland, M. A. O.; Straub, B. F.; Gruber, I.; Rominger, F.; Hofmann, P. *J. Organomet. Chem.* **2001**, *617*−*618* (0), 288−291. (d) Volland, M. A. O.; Rominger, F.; Eisenträger, F.; Hofmann, P. *J. Organomet. Chem.* **2002**, *641* (1−2), 220−226. (e) Volland, M. A. O.; Hansen, S. M.; Rominger, F.; Hofmann, P. *Organometallics* **2004**, *23* (4), 800−816.

(12) (a) Marchenko, A. P.; Koidan, H. N.; Huryeva, A. N.; Zarudnitskii, E. V.; Yurchenko, A. A.; Kostyuk, A. N. *J. Org. Chem.* **2010**, *75* (21), 7141−7145. (b) Marchenko, A. P.; Koidan, H. N.; Pervak, I. I.; Huryeva, A. N.; Zarudnitskii, E. V.; Tolmachev, A. A.; Kostyuk, A. N. *Tetrahedron Lett.* **2012**, *53* (5), 494−496. (c) Nägele, P.; Herrlich, U.; Rominger, F.; Hofmann, P. *Organometallics* **2013**, *32* (1), 181−191.

(13) Brown, C. C.; Plessow, P. N.; Rominger, F.; Limbach, M.; Hofmann, P. *Organometallics* **2014**, *33* (23), 6754−6759.

(14) Kühnel, E.; Shishkov, I. V.; Rominger, F.; Oeser, T.; Hofmann, P. *Organometallics* **2012**, *31* (22), 8000−8011.

(15) Crabtree, R. H.; Felkin, H.; Morris, G. E. *J. Organomet. Chem.* **1977**, *141* (2), 205−215.

(16) Hong, S. H.; Wenzel, A. G.; Salguero, T. T.; Day, M. W.; Grubbs, R. H. *J. Am. Chem. Soc.* **2007**, *129* (25), 7961−7968.

(17) Stumpf, A. W.; Saive, E.; Demonceau, A.; Noels, A. F. *J. Chem. Soc., Chem. Commun.* **1995**, *11*, 1127−1128.

(18) Deng, Q.-H.; Chen, J.; Huang, J.-S.; Chui, S. S.-Y.; Zhu, N.; Li, G.-Y.; Che, C.-M. *Chem. - Eur. J.* **2009**, *15* (41), 10707−10712.

(19) Samojłowicz, C.; Bieniek, M.; Pazio, A.; Makal, A.; Woźniak, K.; Poater, A.; Cavallo, L.; Wójcik, J.; Zdanowski, K.; Grela, K. *Chem. - Eur. J.* **2011**, *17* (46), 12981−12993.

DOI: 10.1021/acs.inorgchem.5b00513
Inorg. Chem. XXXX, XXX, XXX−XXX

(20) (a) Kavitake, S.; Samantaray, M. K.; Dehn, R.; Deuerlein, S.; Limbach, M.; Schachner, J. A.; Jeanneau, E.; Coperet, C.; Thieuleux, C. *Dalton Transactions* **2011**, *40* (46), 12443−12446. (b) Cabrera, J.; Padilla, R.; Bru, M.; Lindner, R.; Kageyama, T.; Wilckens, K.; Balof, S. L.; Schanz, H.-J.; Dehn, R.; Teles, J. H.; Deuerlein, S.; Müller, K.; Rominger, F.; Limbach, M. *Chem. - Eur. J.* **2012**, *18* (46), 14717−14724. (c) Bru, M.; Dehn, R.; Teles, J. H.; Deuerlein, S.; Danz, M.; Müller, I. B.; Limbach, M. *Chem. - Eur. J.* **2013**, *19* (35), 11661−11671.

(21) Songis, O.; Slawin, A. M. Z.; Cazin, C. S. J. *Chem. Commun.* **2012**, *48* (9), 1266−1268.

(22) (a) Warwel, S.; Kätker, H.; Rauenbusch, C. *Angew. Chem., Int. Ed. Engl.* **1987**, *26* (7), 702−703. (b) Rost, A. M. J.; Schneider, H.; Zoller, J. P.; Herrmann, W. A.; Kühn, F. E. *J. Organomet. Chem.* **2005**, *690* (21−22), 4712−4718. (c) Rountree, S. M.; Lagunas, M. C.; Hardacre, C.; Davey, P. N. *Appl. Catal., A* **2011**, *408* (1−2), 54−62.

(23) Behr, A.; Neubert, P.*Applied Homogeneous Catalysis*; Wiley-VCH: Hoboken, NJ, 2012.

(24) Hallman, P. S.; Stephenson, T. A.; Wilkinson, G. Tetrakis-(Triphenylphosphine)Dichloro-Ruthenium(II) and Tris-(Triphenylphosphine)-Dichlororuthenium(II). In *Inorganic Syntheses*; John Wiley & Sons, Inc.: New York, 2007; Vol. *12*, pp 237−240.

(25) (a) Sheldrick, G. M. *SADABS*; Bruker Analytical X-ray-Division: Madison, WI, 2008. (b) Sheldrick, G. M. *Acta Crystallogr., Sect. A: Found. Crystallogr.* **2008**, *64*, 112−122.

DOI: 10.1021/acs.inorgchem.5b00513
Inorg. Chem. XXXX, XXX, XXX−XXX